

# Selective Inhibitors of Human Neuraminidase 3

*Tianlin Guo<sup>‡</sup>, Philipp Dätwyler<sup>§</sup>, Ekaterina Demina<sup>†</sup>, Michele R. Richards<sup>‡</sup>, Peng Ge<sup>‡</sup>, Chunxia Zou<sup>‡</sup>, Ruixiang Zheng<sup>‡</sup>, Anne Fougerat<sup>†</sup>, Alexey V. Pshezhetsky<sup>†</sup>, Beat Ernst<sup>§</sup>, and Christopher W. Cairo<sup>‡\*</sup>*

<sup>‡</sup>Alberta Glycomics Centre and Department of Chemistry, University of Alberta, Edmonton  
Alberta, T6G 2G2, Canada

<sup>§</sup>Department of Pharmaceutical Sciences, Pharmacenter, University of Basel, Klingelbergstrasse  
50, CH-4056 Basel, Switzerland

<sup>†</sup>Division of Medical Genetics, Sainte-Justine University Hospital Research Center, University of  
Montreal, Montréal, Canada

\*Correspondence: University of Alberta, Edmonton, Alberta, T6G 2G2. 780-492-0377 tel., 780-  
492-8231 fax., [ccairo@ualberta.ca](mailto:ccairo@ualberta.ca)

ABSTRACT: Human neuraminidases (NEU) are associated with human diseases including cancer, atherosclerosis, and diabetes. To obtain small molecule inhibitors as research tools for the study of their biological functions, we designed a library of 2-deoxy-2,3-didehydro-*N*-acetylneuraminic acid (DANA) analogues with modifications at C4 and C9 positions. This library allowed us to discover selective inhibitors targeting the human NEU3 isoenzyme. Our most selective inhibitor for NEU3 has a  $K_i$  of  $320 \pm 40$  nM and a 15-fold selectivity over other human neuraminidase isoenzymes. This inhibitor blocks glycolipid processing by NEU3 in vitro. To improve their pharmacokinetic properties, various esters of the best inhibitors were synthesized and evaluated. Finally, we confirmed that our best compounds exhibited selective inhibition of NEU orthologs from murine brain.

## Introduction

Neuraminic acids (also known as sialic acids) form a large family of  $\alpha$ -keto acid monosaccharides containing a nine-carbon backbone.<sup>1</sup> They are diverse in structure and widely distributed among organisms in nature. The most common form of neuraminic acid in humans is Neu5Ac (5-acetamido-3,5-dideoxy-D-glycero-D-galacto-non-2-ulosonic acid).<sup>2</sup> Generally, neuraminic acids are the terminal residues in glycan chains, playing crucial roles in molecular recognition.<sup>3</sup> The neuraminic acid content in human cells is controlled by enzymes including sialyltransferases and neuraminidases (NEU; also known as sialidases).<sup>4</sup> In humans, four neuraminidase isoenzymes have been identified: NEU1, NEU2, NEU3, and NEU4.<sup>5</sup> They exhibit different subcellular localization and show different preferences towards glycan substrates.<sup>5</sup> Abnormal activity of human neuraminidases has been linked to diseases including lysosomal storage disorders,<sup>6,7</sup> cardiovascular diseases,<sup>8,9</sup> and cancer.<sup>10-12</sup> Selective inhibitors of NEU4 have been used to investigate the role of NEU4 in glioblastoma,<sup>13</sup> and NEU1 inhibitors have been employed to study epithelial migration and bacterial adhesion.<sup>14</sup> Thus, isoenzyme-selective inhibitors of human neuraminidases are potential tools to study the biological function of these enzymes.<sup>15</sup>

Although there has been significant efforts to develop potent inhibitors of viral neuraminidases,<sup>16</sup> inhibitors of human neuraminidases are not as thoroughly explored,<sup>15</sup> and most viral neuraminidase inhibitors have only weak or limited activity for the human neuraminidases.<sup>15, 17, 18</sup> The most active viral inhibitor against the human isoenzymes is zanamivir (**6**, Figure 1), which has low micromolar activity for NEU2 and NEU3.<sup>17, 19</sup> Most human neuraminidase inhibitors reported to-date are based on 2-deoxy-2,3-didehydro-*N*-acetylneuraminic acid (DANA, **1**; Figure 1).<sup>15,20</sup> Magesh et al. investigated a series of C9-amide analogues of DANA, and reported a NEU1-

selective inhibitor containing a C9-pentylamide with an  $IC_{50}$  of 10  $\mu$ M (C9-BA-DANA<sup>21</sup>, **2**; Figure 1).<sup>22</sup> Modifications of the C5 and C9 positions of DANA improved potency for DANA analogues against NEU2.<sup>19, 23</sup> Selective inhibitors for NEU2 (**3**, Figure 1) and NEU3 (**4**, Figure 1) were identified in a library of DANA analogs when the glycerol side chain was replaced by oxime- and amino-linked aromatic groups.<sup>24</sup> Inhibitor **3** has a reported  $IC_{50}$  of 86  $\mu$ M against NEU2 with 12-fold selectivity. Inhibitor **4** was the most selective compound reported to date for NEU3 with a 38-fold selectivity ( $IC_{50}$  = 24  $\mu$ M). We previously examined triazole modifications at the C5 and C9 positions in DANA, and found improved potency of C9-triazolyl DANA analogues toward NEU3.<sup>25</sup> When evaluated against the full panel of NEU isoenzymes, C9-4-hydroxymethyltriazolyl DANA (C9-4HMT-DANA, **5**; 500-fold selective,  $K_i$  = 30 nM, Figure 1) turned out to be the most selective inhibitor for NEU4 identified to date. This compound has remained the only reported inhibitor with sub-micromolar activity for any human NEU.<sup>26</sup> We, therefore, considered that a more extensive library of triazole analogs might take advantage of the hypothesized large C9-pocket of NEU3, and could provide selective inhibitors of NEU3 with further improvements in potency. Furthermore, the activity of zanamivir **6** against NEU3 suggested that an appropriate C4 moiety could contribute to increased activity.

In this work, we designed and synthesized a series of compounds featuring a C9-triazolyl group combined with guanidino and other groups at C4. The first series of C9-triazolyl DANA derivatives exhibited remarkably increased potencies relative to the parent compound **1** towards NEU3 and NEU4 (**7**, Figure 1). Although the combination of the best C9-triazolyl fragments with a guanidino group at C4 provided only small gains in potency for NEU3, we found that selectivity for NEU3 over NEU4 was remarkably improved (**8**, Figure 1). The inhibitors presented here

constitute the most potent and selective compounds identified for NEU3 so far. In addition, we have established a rationale for the development of future selective inhibitors of NEU3.

## Results

**Inhibitor Design and Synthesis.** To date, X-ray crystal structure data is only available for human NEU2, including co-crystal data with inhibitors.<sup>27,28</sup> Homology models for NEU3<sup>29-31</sup> have suggested that its glycerol binding pocket is larger than in NEU2. The homology models of NEU3 also indicate that the glycerol side chain interacts with Y179 and Y181. Earlier work reported that large groups, such as a C9-phenyltriazolyl, were tolerated by the C9 pocket of NEU3,<sup>25</sup> but no fragment has been identified which substantially improved potency. We first hypothesized that an appropriate aromatic group at C9 would provide additional interactions and could improve NEU3 potency over other isoenzymes. We therefore explored C9-4-aryl-triazolyl DANA derivatives with variations in electron-donating groups, charge, as well as larger phenyl and phenoxy groups (**7**, Figure 1). We also considered that a guanidino group at C4 could improve activity for NEU2 and NEU3<sup>17, 19</sup> and, therefore, investigated C9-triazolyl DANA derivatives with nitrogen-containing groups at C4, including guanidino, azido, and amino groups.

To prepare analogs with substituted phenyltriazolyl groups at C9, we started from the reported C9-azido-DANA methyl ester (**9**, Scheme 1), which was synthesized from Neu5Ac in 6 steps.<sup>25</sup> The library of triazolyl derivatives **10a-j** was obtained by CuAAC (Cu-catalyzed azide-alkyne cycloaddition) following reported conditions (Scheme 1).<sup>25, 32, 33</sup> Finally, deprotection yielded the test compounds **7a-j**, in moderate to good yields.

For compounds with combined C4,C9-modifications (**8**, Figure 1), two strategies were adopted. Starting from the C9-triazolyl DANA analogue **10h**, a C4-azido group was introduced according to a reported procedure via nucleophilic ring opening of an oxazoline intermediate **11** to yield

compound **12** (Scheme 2).<sup>33</sup> Reduction of the C4-azido of compound **12** via Staudinger reduction provided the C4-amino compound **14**.<sup>34, 35</sup> After deprotection, the C4-azido and C4-amino intermediates **12** and **14** gave the test compounds **13** and **15**. Furthermore, the amino group in **14** was converted to a guanidino group using *N,N'*-di-Boc-1*H*-pyrazole-1-carboxamidine, yielding the final C4, C9-modified test compound **8a** after deprotection. To obtain an alternative polar group at C4, a C4-*N*-alkyl urea compound was prepared by treatment of **14** with 1,1'-carbonyldiimidazole and  $\beta$ -alanine methyl ester. Finally, hydrolysis provided test compound **18**.

An alternative strategy (Scheme 3) allowed preparation of compound **8b** by reversing the order of the modifications at the 4- and 9-position. First, *O*-acetyl protected C4-amino-DANA **19** was prepared as reported.<sup>34</sup> Protection of the amino group with Boc, followed by acetate deprotection (**20**) and subsequent tosylation at C9 (**21**) allowed for displacement to the C9-azido group (**22**).<sup>25</sup> Next, the guanidino group was introduced at C4 to provide compound **23**. Subsequent CuAAC with a biphenyl ethyne allowed for installation of the C9-triazolyl group, forming compound **24**, which gave test compound **8b** after deprotection.

Additional compounds for testing included a small series of C4-amides, prepared starting from compound **19** by treatment with the appropriate anhydride or acyl chloride to yield the amido compounds **25a-d** (Scheme 4) after hydrolysis of the C1-methyl ester with sodium hydroxide. Compounds **1**, **2**, and **6** were also prepared for use in the inhibition assays.

**Inhibition Assays.** To determine the inhibitory potency of the panel of inhibitors against NEU, isoenzymes were prepared either recombinantly or by purification.<sup>24, 26, 29</sup> For the determination of enzyme activity (see Table 1), the fluorogenic neuraminidase substrate, 2'-(4-methylumbelliferyl)- $\alpha$ -D-*N*-acetylneuraminic acid (4MU-NANA) was used.<sup>36, 37</sup> We confirmed that compound **2** acted as a selective inhibitor of NEU1 (IC<sub>50</sub> of 3.4  $\pm$  0.2  $\mu$ M).<sup>22</sup> Compounds **7a-j** with C9-phenyltriazolyl

groups were significantly more potent inhibitors of NEU3 and NEU4 compared to NEU1 and NEU2. For virtually all compounds containing a C9-phenyltriazolyl group we observed single-digit micromolar or better IC<sub>50</sub> values towards NEU3. Compounds with an acidic group (**7h**) or larger aromatic groups (**7i** and **7j**) showed improved activity against NEU3 over those with basic groups (**7a** and **7c**) or neutral electron-withdrawing groups (**7f**). Among all C9-modified DANA analogues, the C9-biphenyltriazolyl DANA **7i** showed the highest potency with an IC<sub>50</sub> of 0.70 ± 0.10 μM and 0.52 ± 0.10 μM towards NEU3 and NEU4, respectively. The activity of **7i** showed distinct preferences, with 40-fold greater potency against NEU3 and NEU4 than for NEU1 or NEU2.

Our library of C4 modifications revealed the importance of the guanidino group for NEU3 selectivity. The comparison of DANA (**1**) and zanamivir (**6**) was consistent with previous reports<sup>17, 19</sup> with potency of 37 ± 6 μM and 7.8 ± 2.0 μM for NEU2 and 7.7 ± 0.8 μM vs 4.0 ± 0.6 μM for NEU3. Decreased potency of 49 ± 8 μM and > 500 μM was found for NEU1 and 8.3 ± 1.0 μM vs 47 ± 6 μM for NEU4. Other nitrogen-containing groups at C4, like azido, amino, or amido moieties (**13**, **15**, **18**, **25**), decreased potency for all isoenzymes. These results are in agreement with previously reported findings as C4-azido- and C4-amino-DANA showed improved potency towards NEU2, and significantly decreased potency towards other isoenzymes.<sup>24</sup> We therefore concluded that a positively charged group of appropriate size at C4 was critical for NEU3 selectivity. Thus, a guanidino group at C4 combined with C9-modification conferred selectivity for NEU3 over NEU4. Selective and potent inhibitors for NEU3 were identified, where compound **8a** (NEU3 IC<sub>50</sub> of 0.6 ± 0.1 μM) showed 40-fold selectivity, and compound **8b** (NEU3 IC<sub>50</sub> of 0.58 ± 0.14 μM) had 10-fold selectivity. Although both **8a** and **8b** demonstrated unprecedented potency for NEU3, we selected **8b** for further studies due to its reduced polarity.

Next, we determined the inhibition constants ( $K_i$ ) of the best inhibitors for their active targets (Table 2). The  $K_i$  results showed a trend similar to the  $IC_{50}$  values. When zanamivir **6** was tested against NEU2, NEU3, and NEU4, we found  $K_i$  values of  $5.7 \pm 1.5 \mu\text{M}$ ,  $0.62 \pm 0.09 \mu\text{M}$ , and  $26 \pm 4 \mu\text{M}$ , respectively. Whereas compound **7i** showed similar  $K_i$  values for NEU3 and NEU4 ( $0.28 \pm 0.04 \mu\text{M}$  and  $0.26 \pm 0.04 \mu\text{M}$ , respectively), the 4-guanidino derivative **8b** exhibited 15-fold selectivity for NEU3 ( $K_i$  for NEU3  $0.32 \pm 0.04 \mu\text{M}$ ; and  $5 \pm 1 \mu\text{M}$  for NEU4). Since NEU3 is known to favor glycolipid substrates over 4MU-NANA,<sup>38</sup> we also tested the inhibitory activity of the best NEU3 inhibitors to block GM3 hydrolysis by the enzyme (Table 3). In comparison with DANA **1**, **7i** showed a higher inhibitory potency for GM3 cleavage catalyzed by NEU3 ( $12 \pm 2 \mu\text{M}$  vs  $54 \pm 10 \mu\text{M}$ ) and NEU4 ( $3.7 \pm 0.7 \mu\text{M}$  vs  $26 \pm 8 \mu\text{M}$ ), and **8b** was 14-fold more potent than DANA (**1**) ( $3.8 \pm 0.5 \mu\text{M}$  vs  $54 \pm 10 \mu\text{M}$ ).

**Pharmacokinetic Evaluation of Active Inhibitors.** For planning future *in vivo* experiments with this series of potent NEU3 inhibitors, their pharmacokinetic properties are critical. Carbohydrate mimetics are typically hydrophilic and are, therefore, often delivered as lipophilic ester prodrugs to improve membrane permeability, where the active principle is released via hydrolysis by esterases.<sup>39, 40</sup> Therefore, C1-esters of inhibitors **1**, **2**, **5**, **7i** and **8b** were prepared. The methyl ester of each compound was obtained after CuAAC as described earlier, whereas elongated aliphatic esters of **7i** were prepared from the C1 methyl ester of **7i** (**7i-OMe**) via transesterification catalyzed by LiBr and DBU.<sup>41</sup> The octanol-water partition coefficients ( $\log P$ ), membrane permeation ( $\log P_e$ ), kinetic solubility, and metabolic stability of the selected compounds were determined.<sup>42</sup> The  $\log P$  values were determined at pH 7.4 using a shake-flask procedure.<sup>43,44</sup> Membrane permeation  $\log P_e$  was determined using a parallel artificial membrane

permeability assay (PAMPA).<sup>45</sup> A summary of the pharmacokinetic parameters is provided in Table 4. A plot of the measured  $\log D_{7.4}$  against  $\log P_e$  is shown in Figure 2 with indications for moderate and high absorption potential.<sup>46</sup> Passive permeability ( $\log P_e$ ) of ester prodrugs is dependent on lipophilicity. In general, the ester prodrugs showed consistently low solubility and time-dependent precipitation. While the solution of the dissolved esters appeared clear after the initial dilution of the DMSO stock with water, turbidity developed after several hours, indicating the formation of precipitates. Because PAMPA required 16 h incubation time, measurements were performed with 10% DMSO.

The passive permeation ( $\log P_e$ ) of all compounds was below the threshold of -6.3, predicting moderate absorption potential (Figure 2). Only the largest aliphatic ester prodrug (**7i-OBu**) reached the lower limit of this threshold. In combination with the low solubility, the compounds are classified as class IV compounds in the biopharmaceutical drug classification system.<sup>47</sup> This class of compounds is highly susceptible to individual transport mechanisms and therefore,<sup>48</sup> we further explored the permeability of the *n*-butyl ester of **7i** (**7i-OBu**) using a colon carcinoma (Caco2) cell-based permeation assay.<sup>49</sup> The threshold for a moderate absorption potential is  $2.0 \times 10^{-6}$  cm s<sup>-1</sup> in the absorptive direction (apical to basolateral; a-b)<sup>42</sup> and was not reached by **7i-OBu**. Additionally, the compound had an efflux ratio of 6.7, predicting active efflux. When the metabolic stability of the prodrug in rat liver microsomes was assessed (Table 5), the hydrolysis of the ester was slow in rat liver microsomes, limiting the release of the active principle. We also determined the stability of **7i-OBu** in human liver microsomes, and found a  $t_{1/2} > 90$  min (see Supporting information). A slow release of the active principle can be beneficial, especially for hydrophilic carbohydrate mimetics to overcome the common problem of fast renal excretion, but in our case the active principle is already lipophilic and the biphenyl moiety is likely prone to oxidation by

cytochromes. In summary, the lead compound **7i-OBu** showed insufficient solubility, a suboptimal efflux ratio and slow permeability in a cell permeation assay, and slow metabolic release of the active principle. Together, these results predict low oral bioavailability without further modification.

**Active Site Models of Human NEUs.** To gain structural insight into the selectivity of active inhibitors, we ran 50-ns molecular dynamics (MD) simulations of **8b** in complex with NEU2, NEU3, and NEU4. NEU models were based on reported X-ray or homology models.<sup>27, 29-31, 50</sup> The starting structures for each simulation are shown in the Supporting Information. Inhibitor **8b** remained bound in the three active sites throughout the MD simulations (Figure 3), and the parent DANA ring in **8b** maintained the ring conformation that mimics the proposed transition state of the oxocarbenium ion intermediate. We analyzed ring conformations of **8b** in the simulations using standard nomenclature for six membered monosaccharides, with C2 being the anomeric carbon (Figure 1, **1**).<sup>51</sup> The population of ring conformations<sup>51</sup> observed for **8b** were found over  $E_5$ - ${}^6H_5$ - ${}^6E$ , and were similar for all three enzymes – with NEU2 centered at  $94^\circ$  ( ${}^6H_5$ ), NEU3 centered at  $106^\circ$  ( ${}^6H_5/{}^6E$ ), and NEU4 centered at  $82^\circ$  ( $E_5/{}^6H_5$ ).<sup>52</sup> For comparison, the ring conformation of DANA **1** bound to NEU2 is  $E_5$  in the co-crystal structure (PDB ID: 1VCU).<sup>53</sup>

We had predicted that large groups at C9 would provide better inhibitors of NEU3 and NEU4 – based on previous inhibitor studies,<sup>25</sup> as well as on previous MD simulations.<sup>54</sup> One reason for this difference in the C9 binding pocket is found in the P267–G275 loop of NEU2, which contains an extra amino acid in comparison to the same loops in NEU3 and NEU4. In Figure 3, a key residue on this loop is shown for each enzyme – Q270 for NEU2, H277 for NEU3, and W274 for NEU4. In NEU2, Q270 forms a H-bond with the triazole of **8b** for 10% of the simulation (Figure 3-A,

Supporting Information). Furthermore, the triazole is within 7 Å of Q270 for 30% of the simulation ( $6.4 \pm 0.6$  Å, average distance between triazole N3 of **8b** and carbonyl oxygen of Q270). To accommodate the large biphenyl-triazole, the P267–G275 loop changes position, and moves Q270 in closer contact with the carboxylate of **8b** ( $5.5 \pm 0.8$  Å, average distance between carboxylate of **8b** and terminal amide of Q270, as shown in Figure 3-A). The comparable residue in NEU3 – H277 – forms a H-bond with the triazole for 17% of the simulation and is within 7 Å of the triazole for 100% of the time (Figure 3-B,  $4.7 \pm 0.4$  Å, average distance between triazole N3 of **8b** and carbonyl oxygen of H277). While W274 in NEU4 does not form any H-bonds with **8b**, it remains within 7 Å of the biphenyl group of **8b** for 100% of the simulation (Figure 3-C,  $3.8 \pm 0.6$  Å, average distance between carbonyl oxygen of W274 and the carbon *ortho* to the triazole in **8b**). However, this relatively close contact is not sufficient to prevent rotation of the biphenyl-triazole substituent. The flexibility of **8b** in the active site of NEU4 could be one reason for the higher inhibitory potency for NEU3 over NEU4.

Looking at the IC<sub>50</sub> values for **1** and **6**, we sought an explanation from our MD simulations for the selectivity the C4 guanidine provides for NEU3 over NEU4. The C4 guanidine of **8b** forms the most highly populated H-bonds between the inhibitor and NEU3. The H-bond to E43 is populated for 92% of the simulation (Figure 3-B), whereas the comparable H-bonds in NEU2 and NEU4 are only populated for 47% (to E39, Figure 3-A) and 52% (to E41, Figure 3-C) of the simulation, respectively (see Supporting Information). Additionally, there is a water bridge between **8b** and D50 of NEU3 that is populated for 88% of the simulation. None of the water bridges in simulations with **8b** and NEU2 or NEU4 are occupied for as much of the simulation time (Supporting Information). Thus, we propose that the guanidine moiety displaces an ordered

water from the C4 pocket in the NEU3 active site. In contrast, NEU2 and NEU4 are not able to maintain contacts to this group.

**Activity of Inhibitors Against Murine NEU Orthologs.** In order to confirm the selectivity of our active NEU3 inhibitors *in vivo* against the mouse orthologues; we assayed neuraminidase activity in the tissues of previously described gene-targeted mouse strains deficient in NEU1 (*neu1*<sup>-/-</sup>), NEU3 (*neu3*<sup>-/-</sup>) and NEU4 (*neu4*<sup>-/-</sup>),<sup>55,56,57</sup> respectively. We also produced a mouse line with a double NEU3/NEU4 deficiency (*neu3*<sup>-/-</sup> *neu4*<sup>-/-</sup>) by cross-breeding the individual knockouts. As expected, the expression levels of both *neu3* and *neu4* were below the detection limit in the tissues of the *neu3*<sup>-/-</sup> *neu4*<sup>-/-</sup> mice.<sup>55</sup>

We assayed neuraminidase activity in the mouse brain tissues, where comparable amounts of NEU1, NEU3, and NEU4 (and only negligible amounts of NEU2) were previously described in the WT mice.<sup>58</sup> Acidic neuraminidase activity in the WT brain homogenate, assayed using the 4MU-NANA substrate, was reduced to ~85% in the presence of 10 μM **8b** and to ~60% in the presence of 50 μM **7i**, suggesting that both NEU3 and NEU4 isoenzymes contribute approximately 10–15% of the net brain neuraminidase activity against 4MU-NANA. Further increase of **7i** to 150 μM did not reduce activity, indicating that even at this concentration the compound did not inhibit mouse NEU1 (Figure 4-A). In contrast, the residual neuraminidase activity levels measured in the brain tissues of NEU1-deficient mice in the presence of saturating concentrations of **8b** and **7i** were drastically different: **8b** reduced the activity to about ~60% of that measured in the absence of inhibitors, whereas **7i** completely inhibited the activity (Figure 4-D). In the brain of NEU3-deficient mice only **7i** could reduce the activity by approximately 20%, which corresponded to the NEU4 fraction of the activity, the rest being NEU1 (Figure 4-B). Finally, both **8b** and **7i** failed to

cause any inhibition of neuraminidase activity in the brain homogenates of NEU3/NEU4 double knockout mice where all activity was presumed to come from the NEU1 isoenzyme (Figure 4-C). Together, our data confirm that the **8b** and **7i** can discriminate between isoforms of mammalian neuraminidases in tissues and could be used to target the specific isozymes *in vivo*.

## Discussion

In glycobiology, human neuraminidases constitute an important family of enzymes,<sup>59</sup> since they play crucial roles in numerous biological processes through the control of sialoglycoconjugate catabolism. Potent and selective chemical inhibitors represent valuable tools for investigating the biological functions of these enzymes. Viral neuraminidase inhibitors with low nanomolar activities have seen successful clinical application as anti-viral drugs.<sup>16</sup> However, there remains a need for strategies to generate selective and potent inhibitors for human neuraminidases.

In this work, we identified selective inhibitors of NEU3 from a small library of DANA analogues with modifications at C4 and C9. Based on previously reported structure-activity relationship studies (SAR) and protein structures, we hypothesized that large aromatic groups at C9 could improve potency against NEU3. In our study, C9 modifications not only significantly improved the potency towards NEU3 but also for NEU4. Furthermore, the inhibitory profile of zanamivir **6** towards human neuraminidases encouraged us to also study the effects of C4-modifications. Surprisingly, among all the nitrogen-containing groups we tested, only the guanidino group showed significant improvements. Although compounds bearing a C4-guanidino group and C9-modification only slightly improved potency towards NEU3, this modification substantially decreased the potency towards NEU4. Moreover, compound **8b**, with a biphenyltriazolyl group at C9 and a guanidino group at C4, showed slightly improved potency over **7i**, which had only a

biphenyltriazolyl group at C9. The selectivity of compound **8a**, which bears a 4-carboxylphenyltriazolyl group at C9 and a guanidino group at C4, for NEU3 may be due to the presence of a carboxylate on the aryl group.

Analysis of the pharmacokinetic properties of our lead compounds **7i** and **8b** suggested that they are unlikely to be orally bioavailable. Permeability assays using artificial membranes (PAMPA) showed that the parent compounds **7i** and **8b**, and most of the C1-ester prodrugs were not sufficiently permeable for oral bioavailability. The lower threshold of sufficient permeability in PAMPA to predict moderate oral bioavailability is a  $\log P_e$  of -6.3.<sup>46</sup> Only the most lipophilic *n*-butyl ester **7i-OBu** reached this limit with a  $\log P_e = -6.5 \pm 0.4$ . The low solubility of 3 to 5  $\mu\text{g mL}^{-1}$  further contributes to poor pharmacokinetic properties. Furthermore, cell permeability data for **7i-OBu** suggested that the compound was likely subject to active efflux, which adds to the limitation of its bioavailability. Finally, the examination of the liver microsome stability of **7i-OBu** showed that the ester was only slowly hydrolyzed. In summary, esterification did not improve pharmacokinetic properties sufficiently to allow for oral bioavailability. Future studies should implement modifications of the active principle to reduce the risk of insufficient permeability and solubility.

Molecular modeling studies provided insight into the structural elements responsible for selectivity between NEU3 and NEU4 relative to other isoenzymes. Since only crystal structures for NEU2 were available, we used homology models to study NEU3 and NEU4. Our previous hypothesis of larger C9-pockets available on both NEU3 and NEU4 explained the activity of compounds such as **7i**, which gained substantial activity over DANA (**1**) for both NEU3 and NEU4. Inhibitors of both NEU3 and NEU4 could be useful agents as these enzymes are known to act on similar substrates and may compensate for each other in vivo.<sup>60</sup> The selectivity over NEU1 and

NEU2 can be attributed to the limited size of their C9-pockets. Furthermore, our models provided a rationale for the observed selectivity of inhibitors with a C4-guanidino group (**6**, **8a**, **8b**) for NEU3. The inclusion of the C4-guanidino group confers a notable improvement in activity against NEU3, and our data suggested this could be due to the displacement of an ordered water in the active site.<sup>61</sup> The absence of a comparable ordered water molecule prevented these compounds from gaining similar activity against NEU4. In general, the C4-guanidino modification reduced NEU4 activity relative to the parent structures (compare **1** and **6**; **7h** and **8a**; **7i** and **8b**). This finding provides an important design principle for future NEU3 inhibitor design.

## Conclusion

In this study, we demonstrated that the scaffold of the neuraminidase inhibitor DANA **1** can be used as a starting point for the generation of new potent and selective inhibitors of human neuraminidase isoenzymes. First, aryltriazolyl groups at C9 greatly improved the potency of inhibitors towards NEU3 and NEU4; and second, the inclusion of a guanidino group at C4 provided selectivity between NEU3 and NEU4 revealing a clear strategy for the design of inhibitors with improved selectivity for NEU3 with sub-micromolar potencies. These inhibitors may be adapted as useful tools to study the biological function of human neuraminidases. In summary, our data confirmed that divergent structural features of the active site of human neuraminidase isoenzymes allowed identification of selective and potent inhibitors of this important family of human glycosidases. Future studies will address the activity of these compounds *in vivo*, and provide new tools for dissecting the specific biological roles of NEU isoenzymes.

## Experimental Section

**General Synthetic Procedures.** All reagents and solvents were purchased from Sigma-Aldrich unless otherwise noted and used without further purification. Reactions were monitored with TLC (Merck TLC Silica gel 60 F<sub>254</sub>) and spots were visualized under UV light (254 nm) or by charring with 0.5 % H<sub>2</sub>SO<sub>4</sub>/EtOH. Compounds were purified by flash column chromatography with silica gel (SiliCycle SiliaFlash® F60, 40-63 µm particle size) or recrystallization with solvents specified in the corresponding experiments. Proton (<sup>1</sup>H) and carbon (<sup>13</sup>C) NMR spectra were recorded on Varian 400 (400 MHz for <sup>1</sup>H; 100 MHz for <sup>13</sup>C), Varian 500 (500 MHz for <sup>1</sup>H; 125 MHz for <sup>13</sup>C) or Varian 700 (700 MHz for <sup>1</sup>H; 175 MHz for <sup>13</sup>C). High-resolution mass spectrometry (HR-MS) analysis was performed on Agilent Technologies 6220 TOF spectrometer. Purity of all final products used for inhibitor assays and pharmacokinetic studies was determined to be ≥95% by HPLC or LC-MS (see Supporting Information for details).

**5-Acetamido-2,6-anhydro-3,5-dideoxy-D-glycero-D-galacto-non-2-enonic acid (DANA, 1)** was synthesized as previously reported.<sup>25</sup> <sup>1</sup>H NMR (500 MHz, CD<sub>3</sub>OD) δ 5.67 (d, *J* = 2.3 Hz, 1H, H-3), 4.36 (dd, *J* = 8.6, 2.3 Hz, 1H, H-4), 4.10 (dd, *J* = 10.9, 1.1 Hz, 1H, H-6), 3.99 (dd, *J* = 10.9, 8.6 Hz, 1H, H-5), 3.87 (ddd, *J* = 9.1, 5.4, 3.1 Hz, 1H, H-8), 3.80 (dd, *J* = 11.4, 3.1 Hz, 1H, H-9), 3.65 (dd, *J* = 11.4, 5.4 Hz, 1H, H-9'), 3.52 (dd, *J* = 9.1, 1.1 Hz, 1H, H-7), 2.02 (s, 3H, COCH<sub>3</sub>). <sup>13</sup>C NMR (125 MHz, CD<sub>3</sub>OD) δ 174.68, 170.02 (2 × C=O), 149.95 (C-2), 108.34 (C-3), 77.24 (C-6), 71.29 (C-8), 70.22 (C-7), 68.70 (C-4), 64.94 (C-9), 51.96 (C-5), 22.82 (COCH<sub>3</sub>). HR-MS (ESI) calcd. for C<sub>11</sub>H<sub>16</sub>NO<sub>8</sub> [M-H]<sup>-</sup>, 290.0876; found 290.0879

**Methyl-5-acetamido-2,6-anhydro-3,5-dideoxy-D-glycero-D-galacto-non-2-enonate (DANA-OMe, 1-OMe)** was synthesized as previously reported.<sup>25</sup> <sup>1</sup>H NMR (500 MHz, D<sub>2</sub>O) δ 6.13 (d, *J* = 2.4 Hz, 1H, H-3), 4.60 (dd, *J* = 9.0, 2.4 Hz, 1H, H-4), 4.36 (d, *J* = 10.9 Hz, 1H, H-6), 4.17 (dd, *J*

= 10.8, 9.0 Hz, 1H, H-5), 4.00 (ddd,  $J = 9.0, 6.0, 2.7$  Hz, 1H, H-8), 3.95 (dd,  $J = 11.9, 2.7$  Hz, 1H, H-9), 3.90 (s, 3H, COOCH<sub>3</sub>), 3.77 – 3.71 (m, 2H, H-7, H-9), 2.15 (s, 3H, COCH<sub>3</sub>). <sup>13</sup>C NMR (125 MHz, D<sub>2</sub>O)  $\delta$  175.78, 165.30 (2  $\times$  C=O), 144.37 (C-2), 113.54 (C-3), 77.09 (C-6), 70.84 (C-8), 68.92 (C-7), 68.02 (C-4), 63.99 (C-9), 53.91 (COOCH<sub>3</sub>), 50.59 (C-5), 23.07 (COCH<sub>3</sub>). HR-MS (ESI) calcd. for C<sub>12</sub>H<sub>19</sub>NNaO<sub>8</sub> [M+Na]<sup>+</sup>, 328.1008; found 328.1006.

**5-Acetamido-9-pentanamido-2,6-anhydro-3,5-dideoxy-D-glycero-D-galacto-non-2-enonic acid (C9-BA-DANA, 2)** was synthesized as previously reported.<sup>22</sup> <sup>1</sup>H NMR (500 MHz, CD<sub>3</sub>OD)  $\delta$  5.93 (d,  $J = 1.7$  Hz, 1H, H-3), 4.43 (dd,  $J = 8.6, 1.7$  Hz, 1H, H-4), 4.18 (d,  $J = 10.8$  Hz, 1H, H-6), 4.02 – 3.95 (m, 1H, H-5), 3.95 – 3.87 (m, 1H, H-8), 3.59 (dd,  $J = 13.9, 2.9$  Hz, 1H, H-9), 3.43 (d,  $J = 9.0$  Hz, 1H, H-7), 3.32 – 3.27 (m, 1H, H-9'), 2.22 (t,  $J = 7.6$  Hz, 2H,  $\alpha$ -CH<sub>2</sub>), 2.03 (s, 3H, COCH<sub>3</sub>), 1.64 – 1.54 (m, 2H,  $\beta$ -CH<sub>2</sub>), 1.35 (dd,  $J = 15.0, 7.5$  Hz, 2H,  $\gamma$ -CH<sub>2</sub>), 0.92 (t,  $J = 7.4$  Hz, 3H,  $\delta$ -CH<sub>3</sub>). <sup>13</sup>C NMR (126 MHz, CD<sub>3</sub>OD)  $\delta$  177.26, 174.88 (N-C=O), 165.81 (C-1), 145.81 (C-2), 113.17 (C-3), 77.79 (C-6), 71.50 (C-7), 70.24 (C-4), 68.03 (C-8), 51.97 (C-5), 44.40 (C-9), 36.87 (C- $\alpha$ ), 29.28 (C- $\beta$ ), 23.44 (C- $\gamma$ ), 22.86 (COCH<sub>3</sub>), 14.22 (C- $\delta$ ). HRMS (ESI) calcd. for C<sub>16</sub>H<sub>25</sub>N<sub>2</sub>O<sub>8</sub> [M-H]<sup>-</sup>, 373.1616; found 373.1614.

**Methyl-5-acetamido-9-pentanamido-2,6-anhydro-3,5-dideoxy-D-glycero-D-galacto-non-2-enonate (C9-BA-DANA-OMe, 2-OMe)** was synthesized as previously reported.<sup>22</sup> <sup>1</sup>H NMR (500 MHz, CD<sub>3</sub>OD)  $\delta$  5.93 (d,  $J = 2.4$  Hz, 1H, H-3), 4.43 (dd,  $J = 8.8, 2.4$  Hz, 1H, H-4), 4.19 (d,  $J = 10.6$  Hz, 1H, H-6), 3.98 (dd,  $J = 10.6, 8.8$  Hz, 1H, H-5), 3.94 – 3.89 (m, 1H, H-8), 3.77 (s, 3H, COOCH<sub>3</sub>), 3.59 (dd,  $J = 14.0, 3.1$  Hz, 1H, H-9), 3.42 (d,  $J = 9.1$  Hz, 1H, H-7), 3.31 (m, 1H, H-9'), 2.23 (t,  $J = 7.6$  Hz, 2H,  $\alpha$ -CH<sub>2</sub>), 2.03 (s, 3H, COCH<sub>3</sub>), 1.64 – 1.54 (m, 2H,  $\beta$ -CH<sub>2</sub>), 1.40 – 1.30 (m, 2H,  $\gamma$ -CH<sub>2</sub>), 0.93 (t,  $J = 7.4$  Hz, 3H,  $\delta$ -CH<sub>3</sub>). <sup>13</sup>C NMR (125 MHz, CD<sub>3</sub>OD)  $\delta$  177.31, 174.90, 164.34 (3  $\times$  C=O), 145.18 (C-2), 113.65 (C-3), 77.97 (C-6), 71.50 (C-7), 70.19 (C-4),

67.90 (C-8), 52.90 (COOCH<sub>3</sub>), 52.01 (C-5), 44.49 (C-9), 36.86 (C- $\alpha$ ), 29.27 (C- $\beta$ ), 23.44 (C- $\gamma$ ), 22.85 (COCH<sub>3</sub>), 14.24 (C- $\delta$ ). HRMS (ESI) calcd. for C<sub>17</sub>H<sub>29</sub>N<sub>2</sub>O<sub>8</sub> [M +H]<sup>+</sup>, 389.1924; found 389.1909.

**5-Acetamido-2,6-anhydro-4-guanidino-3,4,5-trideoxy-D-glycero-D-galacto-non-2-enonic acid (zanamivir, 6)** was synthesized as previously reported.<sup>62, 63</sup> <sup>1</sup>H NMR (500 MHz, D<sub>2</sub>O)  $\delta$  5.70 (d,  $J$  = 1.9 Hz, 1H, H-3), 4.54 (dd,  $J$  = 9.3, 1.9 Hz, 1H, H-4), 4.46 (m, 1H, H-6), 4.29 (dd,  $J$  = 10.5, 9.3 Hz, 1H, H-5), 4.02 (ddd,  $J$  = 9.1, 6.2, 2.5 Hz, 1H, H-8), 3.96 (dd,  $J$  = 11.9, 2.5 Hz, 1H, H-9), 3.77 – 3.69 (m, 2H, H-7, H-9'), 2.11 (s, 3H, COCH<sub>3</sub>). <sup>13</sup>C NMR (125 MHz, D<sub>2</sub>O)  $\delta$  175.38, 170.10 (2  $\times$  C=O), 157.99 (C=N), 150.19 (C-2), 104.79 (C-3), 76.33 (C-6), 70.74 (C-8), 69.11 (C-7), 64.03 (C-9), 52.11 (C-4), 48.71 (C-5), 22.93 (COCH<sub>3</sub>). HR-MS (ESI) calcd. for C<sub>12</sub>H<sub>21</sub>N<sub>4</sub>O<sub>7</sub> [M+H]<sup>+</sup>, 333.1405; found 333.1400

**General Procedure of CuAAC Reaction and Hydrolysis of Methyl Ester.** To a solution of methyl 5-acetamido-9-azido-2,6-anhydro-3,5-dideoxy-D-glycero-D-galacto-non-2-enonate (**9**)<sup>25</sup> (1 eq) and the corresponding alkyne (1.5 eq) in THF-H<sub>2</sub>O (2:1), sodium L-ascorbate (0.5 eq) and copper (II) sulfate (0.5 eq) were added sequentially. The reaction mixture was kept stirring at room temperature and monitored by TLC until no azide remained. Silica gel was then added to the reaction mixture and the solvent was removed under reduced pressure. The residue was separated by flash chromatography to provide the desired products with yields of 42%-88%. To hydrolyze the C1-methyl ester, the product was dissolved in MeOH, and 0.5 M NaOH was added. The mixture was kept stirring at room temperature. After completion, the pH of the solution was adjusted to 2 with Amberlite IR-120 (H<sup>+</sup>). The solution was filtered, concentrated and purified by flash chromatography or recrystallization to provide the desired products with yields of 45%-88%.

**5-Acetamido-9-(4-(dimethylamino)phenyl)-2,6-anhydro-3,5-dideoxy-D-glycero-D-galacto-non-2-enonic acid (7a).** Compound **7a** was prepared as described above in 62% yield (two steps, 86 mg). <sup>1</sup>H NMR (500 MHz, CD<sub>3</sub>OD) δ 8.11 (s, 1H, triazole-H), 7.64 (d, *J* = 8.9 Hz, 2H, Ar-H), 6.81 (d, *J* = 8.9 Hz, 2H, Ar-H), 5.90 (d, *J* = 2.3 Hz, 1H, H-3), 4.49 (dd, *J* = 14.0, 7.5 Hz, 1H, H-9'), 4.40 (dd, *J* = 8.7, 2.3 Hz, 1H, H-4), 4.31 – 4.25 (m, 1H, H-8), 4.14 (dd, *J* = 10.9, 1.0 Hz, 1H, H-6), 3.99 (dd, *J* = 10.9, 8.7 Hz, 1H, H-5), 3.41 (dd, *J* = 9.2, 1.0 Hz, 1H, H-7), 2.96 (s, 6H, N(CH<sub>3</sub>)<sub>2</sub>), 1.99 (s, 3H, COCH<sub>3</sub>). <sup>13</sup>C NMR (125 MHz, CD<sub>3</sub>OD) δ 175.16 (C=O), 152.12, 127.59, 120.10, 113.93 (Ar-C), 149.18 (triazole-C4), 121.83 (triazole-C5), 77.67 (C-6), 71.23 (C-7), 69.79 (C-4), 68.01 (C-8), 55.13 (C-9), 51.96 (C-5), 40.78 (N-CH<sub>3</sub>), 22.65 (COCH<sub>3</sub>). HR-MS (ESI) calcd. for C<sub>21</sub>H<sub>26</sub>N<sub>5</sub>O<sub>7</sub> [M-H]<sup>-</sup>, 460.1832; found 460.1834.

**5-Acetamido-9-(4-acetamidophenyl)-2,6-anhydro-3,5-dideoxy-D-glycero-D-galacto-non-2-enonic acid (7b).** Compound **7b** was prepared as above in 65% yield (two steps, 90 mg). <sup>1</sup>H NMR (500 MHz, CD<sub>3</sub>OD) δ 8.28 (s, 1H, triazole-H), 7.76 (d, *J* = 8.2 Hz, 2H, Ar-H), 7.62 (d, *J* = 8.2 Hz, 2H, Ar-H), 5.70 (s, 1H, H-3), 4.50 (dd, *J* = 13.5, 7.7 Hz, 1H, H-9'), 4.35 (d, *J* = 8.6 Hz, 1H, H-4), 4.30-4.27 (m, 1H, H-8), 4.10 (d, *J* = 10.7 Hz, 1H, H-6), 4.04 – 3.96 (m, 1H, H-5), 3.39 (d, *J* = 7.7 Hz, 1H, H-7), 2.13, 1.98 (2 × s, 3H, 2 × COCH<sub>3</sub>). <sup>13</sup>C NMR (125 MHz, *d*<sub>6</sub>-DMSO) δ 172.10, 168.34, 168.25, 165.18 (4 × C=O), 147.63 (C-2), 145.74 (triazole-C4), 121.67 (triazole-C5), 138.80, 138.69, 125.72, 125.44, 119.20, 119.11 (Ar-C), 108.60 (C-3), 75.66 (C-6), 69.95 (C-7), 68.10 (C-4), 65.90 (C-8), 53.70 (C-9), 50.81 (C-5), 22.97, 22.49 (2 × COCH<sub>3</sub>). HR-MS (ESI) calcd. for C<sub>21</sub>H<sub>24</sub>N<sub>5</sub>O<sub>8</sub> [M-H]<sup>-</sup>, 474.1625; found 474.1636.

**5-Acetamido-9-(4-amidophenyl)-2,6-anhydro-3,5-dideoxy-D-glycero-D-galacto-non-2-enonic acid (7c).** Compound **7c** was prepared as above in 63% yield (two steps, 80 mg). <sup>1</sup>H NMR (500 MHz, CD<sub>3</sub>OD) δ 8.09 (s, 1H, triazole-H), 7.55 (d, *J* = 8.6 Hz, 2H, Ar-H), 6.79 (d, *J* = 8.6 Hz,

2H, Ar-H), 5.88 (d,  $J = 2.4$  Hz, 1H, H-3), 4.82 (dd,  $J = 14.1, 2.6$  Hz, 1H, H-9), 4.48 (dd,  $J = 14.1, 7.6$  Hz, 1H, H-9'), 4.41 (dd,  $J = 8.7, 2.4$  Hz, 1H, H-4), 4.28 (ddd,  $J = 9.5, 7.6, 2.6$  Hz, 1H, H-8), 4.14 (dd,  $J = 10.9, 1.0$  Hz, 1H, H-6), 4.00 (dd,  $J = 10.9, 8.7$  Hz, 1H, H-5), 3.41 (dd,  $J = 9.5, 1.0$  Hz, 1H, H-7), 1.98 (s, 3H, COCH<sub>3</sub>). <sup>13</sup>C NMR (125 MHz, CD<sub>3</sub>OD)  $\delta$  175.13, 166.94 (2  $\times$  C=O), 149.13, 148.42 (Ar-C, triazole-C4), 146.69 (C-2), 127.77, 116.96 (Ar-C), 122.01, 121.94 (Ar-C, triazole-C5), 112.19 (C-3), 77.57 (C-6), 71.24 (C-7), 69.81 (C-4), 68.08 (C-8), 55.14 (C-9), 51.93 (C-5), 22.72 (COCH<sub>3</sub>). HR-MS (ESI) calcd. for C<sub>19</sub>H<sub>22</sub>N<sub>5</sub>O<sub>7</sub> [M-H]<sup>-</sup>, 432.1529; found 432.1513.

**5-Acetamido-9-(4-methylphenyl)-2,6-anhydro-3,5-dideoxy-D-glycero-D-galacto-non-2-enonic acid (7d).** Compound **7d** was prepared as above in 75% yield (two steps, 100 mg). <sup>1</sup>H NMR (500 MHz, CD<sub>3</sub>OD)  $\delta$  8.24 (s, 1H, triazole-H), 7.68 (d,  $J = 8.0$  Hz, 2H, Ar-H), 7.22 (d,  $J = 8.0$  Hz, 2H, Ar-H), 5.79 (s, 1H, H-3), 4.50 (dd,  $J = 13.9, 7.4$  Hz, 1H, H-9'), 4.39 (d,  $J = 8.2$  Hz, 1H, H-4), 4.29 (brs, 1H, H-8), 4.13 (d,  $J = 10.9$  Hz, 1H, H-6), 4.06 – 3.97 (m, 1H, H-5), 3.42 (d,  $J = 9.0$  Hz, 1H, H-7), 2.34 (s, 3H, PhCH<sub>3</sub>), 1.98 (s, 3H, COCH<sub>3</sub>). <sup>13</sup>C NMR (125 MHz, CD<sub>3</sub>OD)  $\delta$  175.00 (C=O), 148.64 (triazole-C4), 123.08 (triazole-C5), 139.31, 130.58, 129.01, 126.62 (Ar-C), 110.40 (C-3), 77.27 (C-6), 71.24 (C-7), 69.84 (C-4), 68.35 (C-8), 55.16 (C-9), 51.95 (C-5), 22.76 (COCH<sub>3</sub>), 21.31 (PhCH<sub>3</sub>). HR-MS (ESI) calcd. for C<sub>20</sub>H<sub>23</sub>N<sub>4</sub>O<sub>7</sub> [M-H]<sup>-</sup>, 431.1567; found 431.1568.

**5-Acetamido-9-(4-methoxyphenyl)-2,6-anhydro-3,5-dideoxy-D-glycero-D-galacto-non-2-enonic acid (7e).** Compound **7e** was prepared as above in 59% yield (two steps, 80 mg). <sup>1</sup>H NMR (500 MHz, CD<sub>3</sub>OD)  $\delta$  8.20 (s, 1H, triazole-H), 7.72 (d,  $J = 8.9$  Hz, 2H, Ar-H), 6.97 (d,  $J = 8.9$  Hz, 2H, Ar-H), 5.77 (d,  $J = 2.0$  Hz, 1H, H-3), 4.49 (dd,  $J = 14.0, 7.6$  Hz, 1H, H-9'), 4.39 (dd,  $J = 8.7, 2.0$  Hz, 1H, H-4), 4.32 – 4.25 (m, 1H, H-8), 4.12 (d,  $J = 10.8$  Hz, 1H, H-6), 4.00 (dd,  $J = 10.8, 8.7$  Hz, 1H, H-5), 3.81 (s, 3H, PhOCH<sub>3</sub>), 3.41 (d,  $J = 9.2$  Hz, 1H, H-7), 1.98 (s, 3H, COCH<sub>3</sub>). <sup>13</sup>C

NMR (125 MHz, CD<sub>3</sub>OD)  $\delta$  174.96 (COCH<sub>3</sub>), 161.27, 128.00, 124.40, 115.37 (Ar-C), 148.49 (triazole-C4), 122.59 (triazole-C5), 109.95 (C-3), 77.20 (C-6), 71.26 (C-7), 69.86 (C-4), 68.38 (C-8), 55.80 (PhOCH<sub>3</sub>), 55.15 (C-9), 51.97 (C-5), 22.74 (COCH<sub>3</sub>). HR-MS (ESI) calcd. for C<sub>20</sub>H<sub>23</sub>N<sub>4</sub>O<sub>8</sub> [M-H]<sup>-</sup>, 447.1516; found 447.1527.

**5-Acetamido-9-(4-fluorophenyl)-2,6-anhydro-3,5-dideoxy-D-glycero-D-galacto-non-2-enonic acid (7f).** Compound **7f** was prepared as above in 62% yield (two steps, 80 mg). <sup>1</sup>H NMR (500 MHz, CD<sub>3</sub>OD)  $\delta$  8.28 (s, 1H, triazole-H), 7.87 – 7.80 (m, 2H, Ar-H), 7.20 – 7.13 (m, 2H, Ar-H), 5.92 (d,  $J$  = 2.4 Hz, 1H, H-3), 4.86 (dd,  $J$  = 14.0, 2.6 Hz, 1H, H-9), 4.51 (dd,  $J$  = 14.0, 7.7 Hz, 1H, H-9'), 4.41 (dd,  $J$  = 8.7, 2.4 Hz, 1H, H-4), 4.29 (ddd,  $J$  = 9.6, 7.7, 2.6 Hz, 1H, H-8), 4.14 (dd,  $J$  = 10.8, 1.1 Hz, 1H, H-6), 3.99 (dd,  $J$  = 10.8, 8.7 Hz, 1H, H-5), 3.43 (dd,  $J$  = 9.6, 1.1 Hz, 1H, H-7), 1.99 (s, 3H, COCH<sub>3</sub>). <sup>13</sup>C NMR (125 MHz, CD<sub>3</sub>OD)  $\delta$  175.15 (C=O), 164.09 (d,  $J$  = 245.9 Hz, Ar-C), 147.63 (triazole-C4), 123.31 (triazole-C5), 128.61 (d,  $J$  = 8.2 Hz, Ar-C), 128.34 (d,  $J$  = 3.2 Hz, Ar-C), 116.77 (d,  $J$  = 22.0 Hz, Ar-C), 112.86 (C-3), 77.70 (C-6), 71.30 (C-7), 69.80 (C-4), 67.95 (C-8), 55.25 (C-9), 51.96 (C-5), 22.64 (COCH<sub>3</sub>). HR-MS (ESI) calcd. for C<sub>19</sub>H<sub>20</sub>FN<sub>4</sub>O<sub>7</sub> [M-H]<sup>-</sup>, 435.1316; found 435.1324.

**5-Acetamido-9-(4-(trifluoromethyl)phenyl)-2,6-anhydro-3,5-dideoxy-D-glycero-D-galacto-non-2-enonic acid (7g).** Compound **7g** was prepared as above in 19% yield (two steps, 40 mg). <sup>1</sup>H NMR (500 MHz, CD<sub>3</sub>OD)  $\delta$  8.44 (s, 1H, triazole-H), 8.02 (d,  $J$  = 8.2 Hz, 2H, Ar-H), 7.72 (d,  $J$  = 8.2 Hz, 2H, Ar-H), 5.95 (d,  $J$  = 2.4 Hz, 1H, H-3), 4.90 (dd,  $J$  = 14.0, 2.6 Hz, 1H, H-9), 4.53 (dd,  $J$  = 14.0, 7.7 Hz, 1H, H-9'), 4.42 (dd,  $J$  = 8.7, 2.4 Hz, 1H, H-4), 4.37 – 4.21 (m, 1H, H-8), 4.16 (dd,  $J$  = 10.8, 1.0 Hz, 1H, H-6), 4.00 (dd,  $J$  = 10.8, 8.7 Hz, 1H, H-5), 3.45 (dd,  $J$  = 9.1, 1.0 Hz, 1H, H-7), 1.99 (s, 3H, COCH<sub>3</sub>). <sup>13</sup>C NMR (125 MHz, CD<sub>3</sub>OD)  $\delta$  175.20 (C=O), 147.04 (triazole-C4), 124.50 (triazole-C5), 135.81 (Ar-C), 130.90 (q,  $J$  = 32.3 Hz, Ar-C), 127.01 (Ar-C), 126.89 (q,  $J$  =

3.8 Hz, Ar-C), 113.43 (C-3), 77.81 (C-6), 71.35 (C-7), 69.80 (C-4), 67.88 (C-8), 55.34 (C-9), 51.95 (C-9), 22.65 (COCH<sub>3</sub>). HR-MS (ESI) calcd. for C<sub>20</sub>H<sub>20</sub>F<sub>3</sub>N<sub>4</sub>O<sub>7</sub> [M-H]<sup>-</sup>, 485.1284; found 485.1282.

**5-Acetamido-9-(4-carboxyphenyl)-2,6-anhydro-3,5-dideoxy-D-glycero-D-galacto-non-2-enonic acid (7h).** Compound **7h** was prepared as above in 74% yield (two steps, 100 mg). <sup>1</sup>H NMR (500 MHz, CD<sub>3</sub>OD) δ 8.42 (s, 1H, triazole-H), 8.06 (d, *J* = 8.5 Hz, 2H, Ar-H), 7.90 (d, *J* = 8.5 Hz, 2H, Ar-H), 5.84 (d, *J* = 1.9 Hz, 1H, H-3), 4.88 (dd, *J* = 14.0, 2.1 Hz, 1H, H-9), 4.54 (dd, *J* = 14.0, 7.6 Hz, 1H, H-9'), 4.43 (dd, *J* = 8.7, 1.9 Hz, 1H, H-4), 4.31 (t, *J* = 7.6 Hz, 1H, H-8), 4.15 (d, *J* = 10.9 Hz, 1H, H-6), 4.03 (dd, *J* = 10.9, 8.7 Hz, 1H, H-5), 3.44 (d, *J* = 7.6 Hz, 1H, H-7), 1.99 (s, 3H, COCH<sub>3</sub>). <sup>13</sup>C NMR (125 MHz, CD<sub>3</sub>OD) δ 175.08, 169.69, 167.90 (3 × C=O), 147.50 (triazole-C4), 124.53 (triazole-C5), 136.19, 131.49, 126.44 (Ar-C), 111.19 (C-3), 77.37 (C-6), 71.31 (C-7), 69.84 (C-4), 68.24 (C-8), 55.29 (C-9), 51.90 (C-5), 22.82 (COCH<sub>3</sub>). HR-MS (ESI) calcd. for C<sub>20</sub>H<sub>21</sub>N<sub>4</sub>O<sub>9</sub> [M-H]<sup>-</sup>, 461.1309; found 461.1316.

**Methyl-5-acetamido-9-(4-biphenyl)-2,6-anhydro-3,5-dideoxy-D-glycero-D-galacto-non-2-enonate acid (7i-OMe).** C1-Methyl ester of **7i** was obtained via CuAAC as described. 69% (71 mg). <sup>1</sup>H NMR (500 MHz, *d*<sub>6</sub>-DMSO) δ 8.46 (s, 1H, triazole-H), 8.19 (d, *J* = 7.4 Hz, 1H, Ar-H), 7.93 (d, *J* = 7.4 Hz, 2H, Ar-H), 7.74 (d, *J* = 7.6 Hz, 2H, Ar-H), 7.70 (d, *J* = 7.0 Hz, 2H, Ar-H), 7.49-7.42 (m, 2H, Ar-H), 7.38-7.32 (m, 1H, Ar-H), 5.81 (s, 1H, H-3), 5.41 (d, *J* = 5.4 Hz, 1H, OH), 5.36 (d, *J* = 4.7 Hz, 1H, OH), 5.10 (s, 1H, NH), 4.77 (d, *J* = 13.4 Hz, 1H, H-9), 4.38-4.25 (m, 2H, H-9', H-4), 4.09-3.95 (m, 2H, H-8, H-6), 3.80 – 3.72 (m, 1H, H-7), 3.69 (s, 3H, COOCH<sub>3</sub>), 1.90 (s, 3H, COCH<sub>3</sub>). <sup>13</sup>C NMR (126 MHz, *d*<sub>6</sub>-DMSO) δ 172.06, 162.12 (2 × C=O), 145.50 (triazole-C4), 143.15 (C-2), 139.56, 139.21, 130.05, 128.92, 127.47, 127.04, 126.45, 125.59 (Ar-C), 122.56 (triazole-C5), 113.36 (C-3), 76.40 (C-6), 69.85 (C-7), 68.00 (C-4), 65.47 (C-8), 53.82 (C-9), 52.06

( $\alpha$ -CH<sub>2</sub>), 50.26 (C-5), 22.52 (COCH<sub>3</sub>). HR-MS (ESI) calcd. for C<sub>26</sub>H<sub>28</sub>N<sub>4</sub>O<sub>7</sub> [M-H]<sup>-</sup>, 509.2031; found 509.2034.

**General Procedure of Transesterification for elongated esters of 7i.** Compound **7i-OMe** was dissolved in corresponding alcohol, then LiBr (5 eq) and DBU (0.5 eq) was added. After stirring at room temperature overnight, solvents were removed under reduced pressure and the residue was purified by flash chromatography to give the desired products (43% - 62%).

**Ethyl-5-acetamido-9-(4-biphenyl)-2,6-anhydro-3,5-dideoxy-D-glycero-D-galacto-non-2-enonate (7i-OEt).** 10 mg (62%). <sup>1</sup>H NMR (700 MHz, *d*<sub>6</sub>-DMSO)  $\delta$  8.48 (s, 1H, triazole-H), 8.22 (d, *J* = 8.1 Hz, 1H, Ar-H), 7.95 (d, *J* = 8.2 Hz, 2H, Ar-H), 7.76 (d, *J* = 8.2 Hz, 2H, Ar-H), 7.72 (d, *J* = 7.7 Hz, 2H, Ar-H), 7.48 (t, *J* = 7.6 Hz, 2H, Ar-H), 7.37 (t, *J* = 7.4 Hz, 1H, Ar-H), 5.82 (d, *J* = 2.4 Hz, 1H, H-3), 5.42 (d, *J* = 6.2 Hz, 1H, OH), 5.38 (d, *J* = 6.5 Hz, 1H, OH), 5.12 (d, *J* = 4.8 Hz, 1H, NH), 4.80 (dd, *J* = 13.9, 2.3 Hz, 1H, H-9), 4.38 – 4.31 (m, 2H, H-9', H-4), 4.19 – 4.13 (m, 2H,  $\alpha$ -CH<sub>2</sub>), 4.06 (ddd, *J* = 14.8, 8.7, 2.6 Hz, 1H, H-8), 3.99 (d, *J* = 10.9 Hz, 1H, H-6), 3.79 – 3.73 (m, 1H, H-5), 3.35 (dd, *J* = 8.7, 5.1 Hz, 1H, H-7), 1.92 (s, 3H, COOCH<sub>3</sub>), 1.21 (t, *J* = 7.1 Hz, 3H,  $\beta$ -CH<sub>3</sub>). <sup>13</sup>C NMR (175 MHz, *d*<sub>6</sub>-DMSO)  $\delta$  172.09, 161.55 (2  $\times$  C=O), 145.49 (triazole-C4), 143.26 (C-2), 139.57, 139.21, 130.08, 128.94, 127.48, 127.06, 126.46, 125.59 (Ar-C), 122.55 (triazole-C5), 113.18 (C-3), 76.47 (C-6), 69.95 (C-7), 68.13 (C-4), 65.49 (C-8), 60.82 ( $\alpha$ -CH<sub>2</sub>), 53.77 (C-9), 50.31 (C-5), 22.53 (COCH<sub>3</sub>), 13.98 ( $\beta$ -CH<sub>3</sub>). HR-MS (ESI) calcd. for C<sub>27</sub>H<sub>31</sub>N<sub>4</sub>O<sub>7</sub> [M-H]<sup>-</sup>, 523.2187; found 523.2186.

**Propyl-5-acetamido-9-(4-biphenyl)-2,6-anhydro-3,5-dideoxy-D-glycero-D-galacto-non-2-enonate (7i-OPr).** 10 mg (63%). <sup>1</sup>H NMR (700 MHz, *d*<sub>6</sub>-DMSO)  $\delta$  8.47 (d, *J* = 5.6 Hz, 1H, triazole-H), 8.22 (d, *J* = 8.2 Hz, 1H, Ar-H), 7.95 (d, *J* = 8.2 Hz, 2H, Ar-H), 7.76 (d, *J* = 8.2 Hz, 2H, Ar-H), 7.72 (d, *J* = 7.5 Hz, 2H, Ar-H), 7.48 (t, *J* = 7.7 Hz, 2H, Ar-H), 7.37 (t, *J* = 7.4 Hz, 1H, Ar-

H), 5.83 (d, J = 2.3 Hz, 1H, H-3), 5.41 (d, J = 6.2 Hz, 1H, OH), 5.38 (d, J = 6.5 Hz, 1H, OH), 5.12 (d, J = 4.7 Hz, 1H, NH), 4.80 (dd, J = 13.9, 2.1 Hz, 1H, H-9), 4.39 – 4.31 (m, 2H, H-9', H-4), 4.10-4.04 (m, 3H,  $\alpha$ -CH<sub>2</sub>, H-8), 3.99 (d, J = 10.8 Hz, 1H, H-6), 3.77 (dd, J = 10.8, 8.6 Hz, 1H, H-5), 1.92 (s, 3H, COOCH<sub>3</sub>), 1.61 (dd, J = 14.1, 7.2 Hz, 2H,  $\beta$ -CH<sub>2</sub>), 0.88 (t, J = 7.2 Hz, 3H,  $\gamma$ -CH<sub>3</sub>). <sup>13</sup>C NMR (175 MHz, *d*<sub>6</sub>-DMSO)  $\delta$  172.09, 161.59 (2  $\times$  C=O), 145.49 (triazole-C4), 143.23 (C-2), 139.57, 139.21, 130.08, 128.94, 127.48, 127.06, 126.46, 125.59 (Ar-C), 122.49 (triazole-C5), 113.14 (C-3), 76.47 (C-6), 69.96 (C-7), 68.20 (C-4), 66.14 (C-8), 65.51( $\alpha$ -CH<sub>2</sub>), 53.76 (C-9), 50.31 (C-5), 22.53 ( $\beta$ -CH<sub>2</sub>), 21.42 (COCH<sub>3</sub>), 10.19 ( $\gamma$ -CH<sub>3</sub>). HR-MS (ESI) calcd. for C<sub>28</sub>H<sub>33</sub>N<sub>4</sub>O<sub>7</sub> [M-H]<sup>-</sup>, 537.2344; found 537.2345.

**Butyl-5-acetamido-9-(4-biphenyl)-2,6-anhydro-3,5-dideoxy-D-glycero-D-galacto-non-2-enonate (7i-OBu).** 7 mg (43%). <sup>1</sup>H NMR (700 MHz, *d*<sub>6</sub>-DMSO)  $\delta$  8.47 (s, 1H, triazole-H), 8.22 (d, J = 8.2 Hz, 1H, Ar-H), 7.97 – 7.93 (m, 2H, Ar-H), 7.78 – 7.74 (m, 2H, Ar-H), 7.73 – 7.70 (m, 2H, Ar-H), 7.49 – 7.46 (m, 2H, Ar-H), 7.39 – 7.35 (m, 1H, Ar-H), 5.82 (d, J = 2.5 Hz, 1H, H-3), 5.40 (d, J = 6.2 Hz, 1H, OH), 5.38 (d, J = 6.5 Hz, 1H, OH), 5.12 (d, J = 4.8 Hz, 1H, NH), 4.81 (dd, J = 13.9, 2.5 Hz, 1H, H-9), 4.39 – 4.31 (m, 2H, H-9', H-4), 4.11 (td, J = 6.5, 1.1 Hz, 2H,  $\alpha$ -CH<sub>2</sub>), 4.07 (tdd, J = 8.7, 6.3, 2.5 Hz, 1H, H-8), 3.99 (d, J = 10.6 Hz, 1H, H-6), 3.77 (dt, J = 10.6, 8.5 Hz, 1H, H-5), 3.36 (dd, J = 8.6, 5.8 Hz, 1H, H-7), 1.92 (s, 3H, COOCH<sub>3</sub>), 1.60 – 1.55 (m, 2H,  $\beta$ -CH<sub>2</sub>), 1.32 (dq, J = 14.7, 7.4 Hz, 2H,  $\gamma$ -CH<sub>2</sub>), 0.86 (t, J = 7.4 Hz, 3H,  $\delta$ -CH<sub>3</sub>). <sup>13</sup>C NMR (175 MHz, *d*<sub>6</sub>-DMSO)  $\delta$  172.10, 161.58 (2  $\times$  C=O), 145.49 (triazole-C4), 143.23 (C-2), 139.84, 139.57, 139.20, 130.09, 128.94, 127.48, 127.05, 126.46, 125.59 (Ar-C), 122.48 (triazole-C5), 113.15 (C-3), 76.50 (C-6), 69.99 (C-7), 68.27 (C-4), 65.49 (C-8), 64.42 ( $\alpha$ -CH<sub>2</sub>), 53.74 (C-9), 50.32 (C-5), 30.03 ( $\beta$ -CH<sub>2</sub>), 22.53 (COCH<sub>3</sub>), 18.59 ( $\gamma$ -CH<sub>2</sub>), 13.48 ( $\delta$ -CH<sub>3</sub>). HR-MS (ESI) calcd. for C<sub>29</sub>H<sub>35</sub>N<sub>4</sub>O<sub>7</sub> [M-H]<sup>-</sup>, 551.2500; found 551.2509.

**5-Acetamido-9-(4-biphenyl)-2,6-anhydro-3,5-dideoxy-D-glycero-D-galacto-non-2-enonic acid (7i).** Compound **7i** was obtained after hydrolysis of **7i-OMe** as described above in 75% (52 mg). <sup>1</sup>H NMR (500 MHz, CD<sub>3</sub>OD) δ 8.34 (s, 1H, triazole-H), 7.88 (d, *J* = 8.1 Hz, 2H, Ar-H), 7.67 (d, *J* = 8.1 Hz, 2H, Ar-H), 7.62 (d, *J* = 7.8 Hz, 2H, Ar-H), 7.42 (t, *J* = 7.6 Hz, 2H, Ar-H), 7.32 (t, *J* = 7.4 Hz, 1H, Ar-H), 5.74 (d, *J* = 1.9 Hz, 1H, H-3), 4.88 (dd, *J* = 13.9, 2.2 Hz, 1H, H-9), 4.52 (dd, *J* = 13.9, 7.7 Hz, H-9'), 4.39 (dd, *J* = 8.7, 1.9 Hz, H-4), 4.37 – 4.21 (m, 1H, H-8), 4.13 (d, *J* = 10.8 Hz, 1H, H-6), 4.02 (dd, *J* = 10.8, 8.7 Hz, 1H, H-5), 3.42 (d, *J* = 9.3 Hz, 1H, H-7), 2.00 (s, 3H, COCH<sub>3</sub>). <sup>13</sup>C NMR (125 MHz, CD<sub>3</sub>OD) δ 174.93, 169.51 (2 × C=O), 149.28 (triazole-C4), 123.47 (triazole-C5), 148.20 (C-2), 142.24, 141.76, 130.84, 129.94, 128.54, 128.48, 127.86, 127.10 (Ar-C), 77.14 (C-6), 71.34 (C-7), 69.83 (C-4), 68.49 (C-8), 55.25 (C-9), 52.00 (C-5), 22.77 (COCH<sub>3</sub>). HR-MS (ESI) calcd. for C<sub>25</sub>H<sub>25</sub>N<sub>4</sub>O<sub>7</sub> [M-H]<sup>-</sup>, 493.1723; found 493.1729.

**5-Acetamido-9-(4-phenoxyphenyl)-2,6-anhydro-3,5-dideoxy-D-glycero-D-galacto-non-2-enonic acid (7j).** Compound **7j** was prepared as above in 40% (two steps, 40 mg). <sup>1</sup>H NMR (500 MHz, CD<sub>3</sub>OD) δ 8.24 (s, 1H, triazole-H), 7.78 (d, *J* = 8.7 Hz, 2H, Ar-H), 7.35 (dd, *J* = 8.7, 7.4 Hz, 2H, Ar-H), 7.12 (t, *J* = 7.4 Hz, 1H, Ar-H), 7.05 – 6.98 (m, 4H, Ar-H), 5.93 (d, *J* = 2.4 Hz, 1H, H-3), 4.85 (dd, *J* = 14.0, 2.5 Hz, 1H, H-9), 4.50 (dd, *J* = 14.0, 7.7 Hz, 1H, H-9'), 4.42 (dd, *J* = 8.7, 2.4 Hz, 1H, H-4), 4.30 (ddd, *J* = 10.0, 7.7, 2.5 Hz, 1H, H-8), 4.16 (m, 1H, H-6), 4.01 (dd, *J* = 10.8, 8.8 Hz, 1H, H-5), 3.47 – 3.41 (m, 1H, H-7), 2.00 (s, 3H, COCH<sub>3</sub>). <sup>13</sup>C NMR (125 MHz, CD<sub>3</sub>OD) δ 175.18, 166.12 (2 × C=O), 158.95, 158.31, 131.00, 128.28, 126.98, 124.77, 120.19, 119.98 (Ar-C), 148.06 (triazole-C4), 123.10 (triazole-C5), 145.90 (C-2), 113.04 (C-3), 77.73 (C-6), 71.32 (C-7), 69.83 (C-4), 67.95 (C-8), 55.25 (C-9), 51.95 (C-5), 22.70 (COCH<sub>3</sub>). HR-MS (ESI) calcd. for C<sub>25</sub>H<sub>25</sub>N<sub>4</sub>O<sub>8</sub> [M-H]<sup>-</sup>, 509.1672; found 509.1674.

**5-Acetamido-9-(4-carboxyphenyl)-2,6-anhydro-4-guanidino-3,4,5-trideoxy-D-glycero-D-galacto-non-2-enonic acid (8a).** To a solution of compound **16** (40 mg) in 1 mL DCM, 100  $\mu$ L TFA was added. The solution was then stirred at room temperature for 2 h. After completion, DCM and TFA were removed under reduced pressure. The residue was dissolved in 2 mL 0.1 N NaOH, and stirred at room temperature for 1 h. After completion, Amberlite IR 120 ( $H^+$ ) was added to the reaction mixture to adjust the pH of the solution to 2. The suspension was then filtered, and the filtrate was concentrated and dissolved in minimum methanol. The desired product was precipitated with ethyl acetate. 10 mg (41%).  $^1H$  NMR (500 MHz,  $D_2O$ )  $\delta$  8.49 (s, 1H, triazole-H), 8.02 (d,  $J = 8.2$  Hz, 2H, Ar-H), 7.93 (d,  $J = 8.2$  Hz, 2H, Ar-H), 5.68 (d,  $J = 2.1$  Hz, 1H, H-3), 4.91 (dd,  $J = 14.4, 2.8$  Hz, 1H, H-9), 4.72 (dd,  $J = 14.4, 6.7$  Hz, 1H, H-9'), 4.48 (dd,  $J = 9.5, 2.1$  Hz, 1H, H-4), 4.46 – 4.41 (m, 1H, H-8), 4.40 (d,  $J = 11.0$  Hz, 1H, H-7), 4.26 (t,  $J = 9.5$  Hz, 1H, H-5), 3.53 (d,  $J = 9.5$  Hz, 1H, H-6), 1.99 (s, 3H,  $COCH_3$ ).  $^{13}C$  NMR (125 MHz,  $D_2O$ )  $\delta$  175.37, 169.94, 163.66 ( $3 \times C=O$ ), 157.96 ( $C=N$ ), 150.14 (C-2), 147.81 (triazole-C4), 124.65 (triazole-C5), 133.00, 130.62, 126.33 (Ar-C), 104.76 (C-3), 76.02 (C-6), 69.79 (C-8), 69.00 (C-7), 54.41 (C-9), 51.83 (C-4), 48.65 (C-5), 22.75 ( $COCH_3$ ). HR-MS (ESI) calcd. for  $C_{21}H_{24}N_7O_8 [M-H]^-$ , 502.1686; found 502.1683.

**Methyl 5-acetamido-9-(4-biphenyl-1H-1,2,3-triazol-1-yl)-4-guanidino-2,6-anhydro-4-[2,3-bis(tert-butoxycarbonyl)guanidino]-3,4,5-trideoxy-D-glycero-D-galacto-non-2-enonate (8b-OMe).** A solution of compound **24** (150 mg) in 3 mL DCM was charged with TFA (300  $\mu$ L) and the solution was stirred at room temperature for 2 h. After completion, DCM and TFA were removed under reduced pressure. The residue was dissolved in 5 mL methanol and cooled to 0  $^{\circ}C$ , followed by addition of NaOMe (54 mg, 5eq). The reaction mixture was stirred at 0  $^{\circ}C$  for 1 h. After completion, Amberlite IR 120 ( $H^+$ ) was added to neutralize the solution. The suspension was

then filtered, and the filtrate was concentrated and purified by flash chromatography to give the desired product. 50 mg (45%). <sup>1</sup>H NMR (500 MHz, CD<sub>3</sub>OD) δ 8.31 (s, 1H, triazole-H), 7.84 (d, J = 8.1 Hz, 2H, Ar-H), 7.62 (d, J = 8.1 Hz, 2H, Ar-H), 7.57 (d, J = 7.5 Hz, 2H, Ar-H), 7.38 (t, J = 7.5 Hz, 2H, Ar-H), 7.29 (t, J = 7.3 Hz, 1H, Ar-H), 5.87 (d, J = 2.0 Hz, 1H, H-3), 4.58 – 4.47 (m, 2H, H-9', H-6), 4.43 (d, J = 10.2 Hz, 1H, H-4), 4.33 – 4.20 (m, 2H, H-8, H-5), 3.72 (s, 3H, COOCH<sub>3</sub>), 3.58 (d, J = 9.0 Hz, 1H, H-7), 1.97 (s, 3H, COCH<sub>3</sub>). <sup>13</sup>C NMR (125 MHz, CD<sub>3</sub>OD) δ 174.57, 163.86 (2 × C=O), 158.95 (C=N), 148.23 (triazole-C4), 146.33, 142.29, 141.69, 130.72, 129.94, 128.58, 128.50, 127.84, 127.11 (Ar-C), 123.71 (triazole-C5), 109.28 (C-3), 77.93 (C-6), 71.21 (C-8), 70.11 (C-7), 55.15 (C-9), 53.07 (COOCH<sub>3</sub>), 51.51 (C-5), 22.69 (COCH<sub>3</sub>). HR-MS (ESI) calcd. for C<sub>27</sub>H<sub>32</sub>N<sub>7</sub>O<sub>6</sub> [M+H]<sup>+</sup>, 550.2414; found 550.2395.

**5-Acetamido-9-(4-biphenyl-1H-1,2,3-triazol-1-yl)-4-guanidino-2,6-anhydro-4-[2,3-bis(tert-butoxycarbonyl)guanidino]-3,4,5-trideoxy-D-glycero-D-galacto-non-2-enonic acid (8b).** A solution of compound **24** (180 mg) in 3 mL DCM was charged with 300 μL TFA and the solution was stirred at room temperature for 2 h. After completion, DCM and TFA were removed under reduced pressure. The residue was dissolved in 3 mL 0.1 N NaOH, and stirred at room temperature for 1 h. After completion, Amberlite IR 120 (H<sup>+</sup>) was added to adjust the pH of the solution to 2. The suspension was then filtered, and the filtrate was concentrated and dissolved in minimum methanol. The desired product was precipitated with ethyl acetate. 10 mg (31%). <sup>1</sup>H NMR (500 MHz, CD<sub>3</sub>OD) δ 8.34 (s, 1H, triazole-H), 7.87 (d, J = 8.1 Hz, 2H, Ar-H), 7.66 (d, J = 8.1 Hz, 2H, Ar-H), 7.61 (d, J = 7.5 Hz, 2H, Ar-H), 7.41 (t, J = 7.6 Hz, 2H, Ar-H), 7.32 (t, J = 7.3 Hz, 1H, Ar-H), 5.89 (s, 1H, H-3), 4.88 (d, J = 14.3 Hz, 1H, H-9), 4.60 – 4.47 (m, 2H, H-9', H-6), 4.42 (d, J = 10.0 Hz, 1H, H-4), 4.28 (m, 2H, H-5, H-8), 3.57 (d, J = 9.0 Hz, 1H, H-7), 1.98 (s, 3H, COCH<sub>3</sub>). <sup>13</sup>C NMR (125 MHz, CD<sub>3</sub>OD) δ 174.56, 165.08 (2 × C=O), 158.96 (C=N), 148.25 (C-

2), 146.68 (triazole-C4), 123.70 (triazole-C5), 142.30, 141.70, 130.71, 129.95, 128.58, 128.50, 127.85, 127.12 (Ar-C), 109.14 (C-3), 77.79 (C-6), 71.21 (C-8), 70.06 (C-7), 55.19 (C-9), 51.53 (C-5), 22.72 (COCH<sub>3</sub>). HR-MS (ESI) calcd. for C<sub>26</sub>H<sub>28</sub>N<sub>7</sub>O<sub>6</sub> [M-H]<sup>-</sup>, 534.2101; found 534.2105.

**2-Methyl-4,5-dihydro-(methyl(7,8-di-*O*-acetyl-9-(4-(methoxycarbonyl)phenyl)-2,6-anhydro-3,4,5-trideoxy-D-glycero-D-talo-non-2-en)onate)[5,4-d]-1,3-oxazole (11).** A solution of compound **10h** (250 mg, 1 eq) in anhydrous pyridine was cooled to 0 °C, followed by dropwise addition of acetic anhydride (230 μL, 4.5 eq). The reaction mixture was allowed to warm to room temperature and kept stirring overnight. After completion, the reaction was quenched with methanol and the solvents were removed under reduced pressure. The residue was dissolved in ethyl acetate and carefully washed with 0.05 M HCl, water, and brine sequentially and dried over Na<sub>2</sub>SO<sub>4</sub>. The solution was then concentrated and purified by flash chromatography, providing a crude fully protected product, which was used in the next step without further purification. 370 mg (*quant.*, crude product). The obtained crude protected product (800 mg, 1 eq, several batches' product of last step) was dissolved in 10 mL ethyl acetate. The solution was warmed to 40 °C and TMSOTf (408 μL, 3 eq) was added dropwise. The resulting solution was kept stirring at 50 °C for 4 hours. After completion, the solution was added to a vigorously stirred cold saturated sodium bicarbonate solution. The aqueous phase was separated and extracted with ethyl acetate. The organic phase was combined, dried over Na<sub>2</sub>SO<sub>4</sub>, concentrated and purified by flash chromatography to give the desired product (430 mg, 60%). <sup>1</sup>H NMR (500 MHz, CD<sub>3</sub>OD) δ 8.49 (s, 1H, triazole-H), 8.03 – 7.97 (d, *J* = 8.5 Hz, 2H, Ar-H), 7.88 (d, *J* = 8.5 Hz, 2H, Ar-H), 6.39 (d, *J* = 4.0 Hz, 1H, H-3), 5.65 – 5.57 (m, 2H, H-7, H-8), 5.22 (dd, *J* = 14.8, 2.6 Hz, 1H, H-9), 4.94 (dd, *J* = 9.5, 4.0 Hz, 1H, H-4), 4.79 (m, 1H, H-9'), 4.02 (t, *J* = 9.5 Hz, 1H, H-5), 3.87, 3.79 (2 × s, 2 × 3H, 2 × COOCH<sub>3</sub>), 3.60 (dd, *J* = 9.5, 2.3 Hz, 1H, H-6), 2.17 (s, 3H, oxazole-CH<sub>3</sub>), 1.97, 1.95

(2 × s, 2 × 3H, 2 × COOCH<sub>3</sub>). <sup>13</sup>C NMR (125 MHz, CD<sub>3</sub>OD) δ 171.55, 171.32, 168.03, 163.34 (4 × C=O), 170.12 (oxazole-O-C=N), 148.09 (triazole-C4), 124.39 (triazole-C5), 147.66 (C-2), 136.30, 131.27, 130.78, 126.55 (Ar-C), 109.05 (C-3), 78.35 (C-6), 74.22 (C-4), 73.52 (C-8), 70.86 (C-7), 62.68 (C-5), 53.27, 52.81 (2 × COOCH<sub>3</sub>), 51.09 (C-9), 20.73, 20.67 (COCH<sub>3</sub>), 14.06 (oxazole-CH<sub>3</sub>). HR-MS (ESI) calcd. for C<sub>26</sub>H<sub>28</sub>N<sub>4</sub>NaO<sub>10</sub> [M+Na]<sup>+</sup>, 579.1703; found 579.1697

**Methyl 5-acetamido-7,8-di-O-acetyl-9-(4-(methoxycarbonyl)phenyl)-2,6-anhydro-4-azido-3,4,5-trideoxy-D-glycero-D-galacto-non-2-enonate (12).** To a solution of compound **11** (430 mg, 1 eq) in dry <sup>t</sup>BuOH, TMSN<sub>3</sub> (507 μL, 5 eq) was added and the resulting solution was stirred at 80 °C under a nitrogen atmosphere for 12 hours. After completion, the solution was cooled to room temperature, concentrated and purified by flash chromatography to give the desired product. 470 mg (*quant.*). <sup>1</sup>H NMR (500 MHz, CD<sub>3</sub>OD) δ 8.51 (s, 1H, triazole-H), 8.07 – 8.02 (m, 2H, Ar-H), 7.92 – 7.87 (m, 2H, Ar-H), 5.97 (d, *J* = 2.2 Hz, 1H, H-3), 5.57-5.56 (dd, *J* = 3.3, 2.2 Hz, 1H, H-4), 5.52 (dt, *J* = 9.1, 2.9 Hz, 1H, H-8), 5.29 (dd, *J* = 14.8, 2.7 Hz, 1H, H-9), 4.71 (dd, *J* = 14.8, 9.1 Hz, 1H, H-9'), 4.49 (dd, *J* = 10.3, 1.9 Hz, 1H, H-6), 4.27 – 4.18 (m, 2H, H-5, H-7), 3.89, 3.80 (2 × s, 2 × 3H, 2 × COOCH<sub>3</sub>), 2.13, 1.93, 1.92 (3 × s, 3 × 3H, 3 × COCH<sub>3</sub>). <sup>13</sup>C NMR (125 MHz, CD<sub>3</sub>OD) δ 173.49, 171.83, 171.42, 168.09, 163.07 (5 × C=O), 147.64 (triazole-C4), 124.51 (triazole-C5), 146.32 (C-2), 136.25, 131.26, 130.85, 126.54 (Ar-C), 109.74 (C-3), 78.44 (C-6), 73.96 (C-8), 69.60 (C-7), 60.46 (C-4), 53.21, 52.74 (2 × COOCH<sub>3</sub>), 51.17 (C-9), 48.39 (C-5), 22.89, 20.88, 20.63 (3 × COCH<sub>3</sub>). HR-MS (ESI) calcd. for C<sub>26</sub>H<sub>29</sub>N<sub>7</sub>NaO<sub>10</sub> [M+Na]<sup>+</sup>, 622.1874; found 622.1866

**5-Acetamido-9-(4-(methoxycarbonyl)phenyl)-2,6-anhydro-4-azido-3,4,5-trideoxy-D-glycero-D-galacto-non-2-enonic acid (13).** A sample of 60 mg of compound **12** was dissolved in 2 mL 0.5 N NaOH, the solution was stirred under room temperature for 1 hour. After completion, Amberlite IR 120 (H<sup>+</sup>) was added to adjust the pH of the solution as 2. The suspension was then

filtered, and the filtrate was concentrated and purified by flash chromatography to give the desired product. 32 mg (66%). <sup>1</sup>H NMR (500 MHz, CD<sub>3</sub>OD) δ 8.43 (s, 1H, triazole-H), 8.06 (d, *J* = 8.2 Hz, 2H, Ar-H), 7.91 (d, *J* = 8.2 Hz, 2H, Ar-H), 5.73 (s, 1H), 4.53 (dd, *J* = 14.0, 7.6 Hz, 1H, H-9'), 4.32 – 4.25 (m, 2H, H-4, H-8), 4.23 (d, *J* = 10.8 Hz, 1H, H-6), 4.18 – 4.10 (m, 1H, H-5), 3.45 (d, *J* = 9.3 Hz, 1H, H-7), 1.98 (s, 3H, COCH<sub>3</sub>). <sup>13</sup>C NMR (125 MHz, CD<sub>3</sub>OD) δ 174.32 (C=O), 147.53 (triazole-C4), 124.47 (triazole-C5), 136.17, 131.48, 126.42 (Ar-C), 104.50 (C-3), 77.02 (C-6), 71.03 (C-8), 69.86 (C-7), 60.23 (C-4), 55.25 (C-9), 48.53 (C-5), 22.78 (COCH<sub>3</sub>). HR-MS (ESI) calcd. for C<sub>20</sub>H<sub>20</sub>N<sub>7</sub>O<sub>8</sub> [M-H]<sup>-</sup>, 486.1373; found 486.1378

**Methyl 5-acetamido-7,8-di-*O*-acetyl-9-(4-(methoxycarbonyl)phenyl)-2,6-anhydro-4-amino-3,4,5-trideoxy-D-glycero-D-galacto-non-2-enonate (14).** To a solution of compound **12** (50 mg, 1 eq) in THF (2 mL), 0.5 N HCl (200 μL, 2 eq) was added, followed by triphenylphosphine (29 mg, 1.1 eq). The resulting mixture was stirred at room temperature overnight. After completion, solvents were removed under reduced pressure and the residue was purified by flash chromatograph, providing the desired product 39 mg (84%). <sup>1</sup>H NMR (500 MHz, CD<sub>3</sub>OD) δ 8.57 (s, 1H, triazole-H), 8.05 (d, *J* = 8.4 Hz, 2H, Ar-H), 7.92 (d, *J* = 8.4 Hz, 2H, Ar-H), 6.06 (d, *J* = 2.3 Hz, 1H, H-3), 5.63 – 5.55 (m, 2H, H-7, H-8), 5.29 – 5.21 (m, 1H, H-9), 4.74 (dd, *J* = 14.7, 8.4 Hz, 1H, H-9'), 4.64 (dd, *J* = 10.0, 1.1 Hz, 1H, H-6), 4.35 (t, *J* = 10.0 Hz, 1H, H-5), 4.15 (dd, *J* = 10.0, 2.3 Hz, 1H, H-4), 3.90, 3.81 (2 × s, 2 × 3H, 2 × COOCH<sub>3</sub>), 2.12, 1.97, 1.95 (3 × s, 3 × 3H, 3 × COCH<sub>3</sub>). <sup>13</sup>C NMR (125 MHz, CD<sub>3</sub>OD) δ 174.28, 171.71, 171.31, 168.15, 162.80 (5 × C=O), 147.66 (triazole-C4), 124.59 (triazole-C5), 147.29, 136.28, 130.84, 126.56 (Ar-C), 107.15 (C-3), 77.96 (C-6), 73.34 (C-8), 69.49 (C-7), 53.34, 52.78 (2 × COOCH<sub>3</sub>), 51.67 (C-4), 51.31 (C-9), 46.73 (C-5), 23.14, 20.89, 20.66 (3 × COCH<sub>3</sub>). HR-MS (ESI) calcd. for C<sub>26</sub>H<sub>31</sub>N<sub>5</sub>NaO<sub>10</sub> [M+Na]<sup>+</sup>, 596.1969; found 596.1967.

**5-acetamido-7,8-di-O-acetyl-9-(4-(methoxycarbonyl)phenyl)-2,6-anhydro-4-amino-3,4,5-trideoxy-D-glycero-D-galacto-non-2-enonic acid (15).** A sample of 35 mg of compound **14** was dissolved in 400  $\mu\text{L}$  1N NaOH and the solution was kept stirring at r.t. for 1 h. After completion, the reaction mixture was adjusted to pH 2 with Amberlite IR 120 ( $\text{H}^+$ ). The suspension was then filtered, and the filtrate was concentrated and dissolved in minimum methanol. The desired product was precipitated with ethyl acetate. 20 mg (71%).  $^1\text{H}$  NMR (500 MHz,  $\text{CD}_3\text{OD}$ )  $\delta$  8.47 (s, 1H, triazole-H), 8.08 (d,  $J = 8.2$  Hz, 2H, Ar-H), 7.94 (d,  $J = 8.2$  Hz, 2H, Ar-H), 5.84 (s, 1H, H-3), 4.89 (d,  $J = 14.4$  Hz, 1H, H-9), 4.56 (dd,  $J = 14.0, 7.5$  Hz, 1H, H-9'), 4.41 – 4.26 (m, 3H, H-8, H-6, H-5), 4.18 (d,  $J = 7.1$  Hz, 1H, H-4), 3.56 (d,  $J = 9.1$  Hz, 1H, H-7), 2.03 (s, 3H,  $\text{COCH}_3$ ).  $^{13}\text{C}$  NMR (125 MHz,  $\text{CD}_3\text{OD}$ )  $\delta$  174.86, 169.48 ( $2 \times \text{C}=\text{O}$ ), 147.50 (triazole-C4), 124.66 (triazole-C5), 136.29, 131.48, 131.25, 126.45 (Ar-C), 103.03 (C-3), 77.01 (C-6), 70.71 (C-8), 70.03 (C-7), 55.19 (C-9), 51.29 (C-4), 47.54 (C-5), 23.03 ( $\text{COCH}_3$ ). HR-MS (ESI) calcd. for  $\text{C}_{20}\text{H}_{22}\text{N}_5\text{O}_8$  [ $\text{M}-\text{H}$ ] $^-$ , 460.1468; found 460.1482.

**Methyl 5-acetamido-9-(4-(methoxycarbonyl)phenyl-1H-1,2,3-triazol-1-yl)-4-[2,3-bis(tert-butoxycarbonyl)guanidino]-7,8-di-O-acetyl-2,6-anhydro-3,4,5-trideoxy-D-glycero-D-galacto-non-2-enonate (16).** To a solution of compound **14** (40 mg, 1 eq) in 2 mL anhydrous DCM, TEA (40  $\mu\text{L}$ , 4 eq) was added. The solution was cooled to 0  $^\circ\text{C}$  and N, N'-Di-Boc-1H-pyrazole-1-carboxamide (42 mg, 2 eq) was added. The reaction mixture was allowed to warm to room temperature and kept stirring overnight. After completion, the reaction was quenched with water and extracted with ethyl acetate. The organic phase was washed with brine, dried over  $\text{Na}_2\text{SO}_4$ , concentrated, and purified by flash chromatography to give the desired product. 40 mg (crude product, 72%).  $^1\text{H}$  NMR (500 MHz,  $\text{CD}_3\text{OD}$ )  $\delta$  8.55 (s, 1H, triazole-H), 8.06 (d,  $J = 8.3$  Hz, 2H, Ar-H), 7.92 (d,  $J = 8.3$  Hz, 2H), 6.00 (d,  $J = 2.3$  Hz, 1H, H-3), 5.58 (d,  $J = 1.5$  Hz, 1H, H-7), 5.56

– 5.52 (m, 1H, H-8), 5.31 (dd,  $J = 14.8, 2.4$  Hz, 1H, H-9), 5.02 (dd,  $J = 10.2, 2.3$  Hz, 1H, H-4), 4.74 (dd,  $J = 14.8, 9.0$  Hz, 1H, H-9'), 4.53 (dd,  $J = 10.2, 1.5$  Hz, 1H, H-6), 4.27 (t,  $J = 10.2$  Hz, 1H, H-5), 3.91, 3.80 ( $2 \times$  s,  $2 \times$  3H,  $2 \times$  COOCH<sub>3</sub>), 2.12, 1.94, 1.85 ( $3 \times$  s,  $3 \times$  3H,  $3 \times$  COCH<sub>3</sub>), 1.51, 1.46 ( $2 \times$  s,  $2 \times$  9H,  $2 \times$  Boc). <sup>13</sup>C NMR (125 MHz, CD<sub>3</sub>OD)  $\delta$  173.57, 171.77, 171.41, 168.07, 164.32, 163.39, 158.01 ( $7 \times$  C=O), 153.82 (C=N), 147.64 (triazole-C4), 124.50 (triazole-C5), 145.61 (C-2), 136.34, 131.27, 131.27, 126.55 (Ar-C), 111.83 (C-3), 84.84, 80.57 ( $2 \times$  <sup>1</sup>Boc–C(CH<sub>3</sub>)<sub>3</sub>), 78.89 (C-6), 74.00 (C-8), 69.87 (C-7), 53.07, 52.74 ( $2 \times$  COOCH<sub>3</sub>), 51.27 (C-9), 50.84 (C-4), 47.90 (C-5), 28.59, 28.26 ( $2 \times$  <sup>1</sup>Boc–C(CH<sub>3</sub>)<sub>3</sub>), 22.77, 20.86, 20.65 ( $3 \times$  COCH<sub>3</sub>). HR-MS (ESI) calcd. for C<sub>37</sub>H<sub>49</sub>N<sub>7</sub>NaO<sub>14</sub> [M+Na]<sup>+</sup>, 838.3235; found 838.3226.

**Methyl 5-acetamido-9-(4-(methoxycarbonyl)phenyl-1H-1,2,3-triazol-1-yl)-4-(3-(3-methoxy-3-oxopropyl)ureido)-7,8-di-O-acetyl-2,6-anhydro-3,4,5-trideoxy-D-glycero-D-galacto-non-2-enonate (17).** A solution of compound **14** (100 mg, 1 eq) and TEA (56 mg, 2 eq) in anhydrous DCM was cooled to 0 °C, and charged with 1,1'-Carbonyldiimidazole (39 mg, 1.2 eq). The reaction mixture was then warmed to room temperature and kept stirring for 2 h until TLC showed consumption of the amine. The solution was then cooled to 0 °C, and the methyl ester of  $\beta$ -alanine (56 mg, 2 eq) was added. The solution was warmed to room temperature and kept stirring overnight. After completion, the reaction was quenched with water, and extracted by ethyl acetate. The organic layer was washed with water, brine, and dried over Na<sub>2</sub>SO<sub>4</sub>. After subsequent concentration, the residue was purified by flash chromatography to give the desired product. 140 mg (*quant.*). <sup>1</sup>H NMR (500 MHz, CD<sub>3</sub>OD)  $\delta$  8.54 (s, 1H, triazole-H), 8.07 (d,  $J = 8.7$  Hz, 2H, Ar-H), 7.92 (d,  $J = 8.7$  Hz, 2H, Ar-H), 5.92 (d,  $J = 2.5$  Hz, 1H, H-3), 5.55 (m, 2H, H-8, H-4), 5.31 (dd,  $J = 14.8, 2.6$  Hz, 1H, H-9), 4.73 (dd,  $J = 14.8, 8.9$  Hz, 1H, H-9'), 4.55 (dd,  $J = 9.9, 2.5$  Hz, 1H, H-7), 4.46 (dd,  $J = 10.2, 2.0$  Hz, 1H, H-6), 4.10 (t,  $J = 10.2$  Hz, 1H, H-5), 3.91, 3.78,

3.66 (3 × s, 3 × 3H, 3 × COOCH<sub>3</sub>), 3.36 (td, *J* = 6.6, 1.9 Hz, 2H, CH<sub>2</sub>), 2.48 (t, *J* = 6.5 Hz, 2H, CH<sub>2</sub>), 2.10, 1.93, 1.87 (3 × s, 3 × 3H, 3 × COCH<sub>3</sub>). <sup>13</sup>C NMR (125 MHz, CD<sub>3</sub>OD) δ 174.12, 173.59, 171.79, 171.41, 168.13, 163.56, 160.42 (7 × C=O), 147.66 (C-2), 145.10 (triazole-C4), 124.46 (triazole-C5), 136.30, 131.26, 130.88, 126.54 (Ar-C), 114.06 (C-1), 79.10 (C-6), 73.99 (C-8), 69.97 (C-7), 52.96, 52.70, 52.15 (3 × COOCH<sub>3</sub>), 51.26 (C-9), 50.38 (C-5), 36.92, 35.64 (CH<sub>2</sub>CH<sub>2</sub>), 22.85, 20.84, 20.59 (COCH<sub>3</sub>). HR-MS (ESI) calcd. for C<sub>31</sub>H<sub>39</sub>N<sub>7</sub>N<sub>6</sub>O<sub>13</sub> [M+Na]<sup>+</sup>, 703.2575; found 703.2571.

**5-Acetamido-9-(4-carboxyphenyl)-2,6-anhydro-4-(3-(2-carboxyethyl)ureido)-3,4,5-trideoxy-D-glycero-D-galacto-non-2-enonic acid (18).** A sample of 140 mg of compound **17** was dissolved in 5 mL 0.1 N NaOH, and stirred at room temperature for 1 h. After completion, the reaction mixture adjusted to pH 2 with the addition of Amberlite IR 120 (H<sup>+</sup>). The suspension was then filtered, and the filtrate was concentrated and dissolved in minimum methanol. The desired product was precipitated with ethyl acetate. 88 mg (77%). <sup>1</sup>H NMR (500 MHz, CD<sub>3</sub>OD) δ 8.44 (s, 1H, triazole-H), 8.07 (d, *J* = 8.4 Hz, 2H, Ar-H), 7.93 (d, *J* = 8.4 Hz, 2H, Ar-H), 5.66 (d, *J* = 1.9 Hz, 1H, H-3), 4.57 (dd, *J* = 9.8, 1.9 Hz, 1H, H-4), 4.52 (dd, *J* = 14.0, 7.7 Hz, 1H, H-9'), 4.30 (dd, *J* = 12.1, 4.8 Hz, 1H, H-8), 4.19 (d, *J* = 10.8 Hz, 1H, H-6), 4.02 (t, *J* = 10.3 Hz, 1H, H-5), 3.44 (d, *J* = 9.3 Hz, 1H, H-7), 3.37 (t, *J* = 6.4 Hz, 2H, CH<sub>2</sub>), 2.46 (t, *J* = 6.4 Hz, 2H, CH<sub>2</sub>), 1.94 (s, 3H, COCH<sub>3</sub>). <sup>13</sup>C NMR (125 MHz, CD<sub>3</sub>OD) δ 175.74, 174.73, 160.76, 169.64 (4 × C=O), 147.51 (triazole-C4), 124.40 (triazole-C5), 136.24, 131.68, 131.45, 126.42 (Ar-C), 109.35 (C-3), 77.81 (C-6), 71.36 (C-8), 69.80 (C-7), 55.31 (C-9), 37.00, 35.78 (CH<sub>2</sub>CH<sub>2</sub>), 22.74 (COCH<sub>3</sub>). HR-MS (ESI) calcd. for C<sub>24</sub>H<sub>27</sub>N<sub>6</sub>O<sub>11</sub> [M-H]<sup>-</sup>, 575.1738; found 575.1738

**Methyl 5-acetylamino-4-(tert-butoxycarbonyl)amino-2,6-anhydro-3,5-dideoxy-D-glycero-D-galacto-non-2-enonate (20).** To a solution of compound **19** (600 mg, 1 eq) and TEA (389 μL,

2 eq) in 20 mL anhydrous DCM at 0 °C, di-*tert*-butyl dicarbonate (456 mg, 1.5 eq) was added dropwise. The mixture was then warmed to room temperature and kept stirring overnight. After completion, solvent was removed and the residue was purified by flash chromatography to give the desired compound in 350 mg (crude product, 47%). The crude product (350 mg, 1 eq) was dissolved in 10 mL methanol, and cooled to 0 °C, followed by addition of NaOMe (92 mg, 3 eq). The solution was kept stirring at 0 °C for 1 h until no starting material remained. The solution was adjusted to pH 2 by addition of Amberlite IR 120 (H<sup>+</sup>). The suspension was then filtered, and the filtrate was concentrated and purified by flash chromatography to give the desired product. 190 mg (71%). <sup>1</sup>H NMR (500 MHz, CD<sub>3</sub>OD) δ 5.82 (d, *J* = 2.2 Hz, 1H, H-3), 4.46 (d, *J* = 10.1 Hz, 1H, H-4), 4.23 (d, *J* = 10.1 Hz, 1H, H-6), 4.05 (t, *J* = 10.1 Hz, 1H, H-5), 3.88 (ddd, *J* = 9.2, 5.4, 2.9 Hz, 1H, H-8), 3.81 (dd, *J* = 11.4, 2.9 Hz, 1H, H-9), 3.65 (dd, *J* = 11.4, 5.4 Hz, 1H, H-9'), 3.58 (dd, *J* = 9.3, 1.1 Hz, 1H, H-7), 1.98 (s, 3H, COOCH<sub>3</sub>), 1.44 (s, 9H, <sup>t</sup>Boc-C(CH<sub>3</sub>)<sub>3</sub>). <sup>13</sup>C NMR (125 MHz, CD<sub>3</sub>OD) δ 174.65, 164.26, 158.35 (3 × C=O), 145.71 (C-2), 112.19 (C-3), 80.56 (<sup>t</sup>Boc-C(CH<sub>3</sub>)<sub>3</sub>), 78.62 (C-6), 71.13 (C-8), 70.00 (C-7), 64.90 (C-9), 52.79 (C-4), 50.26 (C-5), 28.70 (<sup>t</sup>Boc-C(CH<sub>3</sub>)<sub>3</sub>), 22.70 (COCH<sub>3</sub>). HR-MS (ESI) calcd. for C<sub>17</sub>H<sub>29</sub>N<sub>2</sub>O<sub>9</sub> [M+H]<sup>+</sup>, 405.1873; found 405.1875

**Methyl 4-(*tert*-butoxycarbonyl)amino-5-acetylamino-9-(4-methylbenzenesulfonate) -2,6-anhydro-3,5-dideoxy-D-glycero-D-galacto-non-2-enonate (21).** A solution of compound **20** (190 mg, 1 eq) in anhydrous pyridine was cooled down to 0 °C, TsCl (98 mg, 1.1 eq) was then added slowly under stirring. The solution was warmed to room temperature and kept stirring overnight. After completion, the reaction was quenched by methanol. The solution was concentrated and purified by flash chromatography to give the desired product. 200 mg (76%). <sup>1</sup>H NMR (500 MHz, CDCl<sub>3</sub>) δ 7.78 (d, *J* = 8.1 Hz, 2H, Ar-H), 7.33 (d, *J* = 8.1 Hz, 2H, Ar-H), 6.93, 5.23, 5.11, 3.59 (4 × d, 4H, 2 × NH, 2 × OH), 5.82 (d, *J* = 2.3 Hz, 1H, H-3), 4.55 (td, *J* = 9.6, 2.2 Hz, 1H, H-8), 4.40-

4.31 (m, 1H, H-6), 4.21-4.17 (m, 1H, H-5), 4.15-4.11 (m, 2H, H-9', H-4), 4.01-3.95 (m, 1H, H-9'), 3.71 (s, 3H, COOCH<sub>3</sub>), 3.56 – 3.48 (m, 1H, H-7), 2.43 (s, 3H, PhCH<sub>3</sub>), 2.00 (s, 3H, COCH<sub>3</sub>), 1.42 (s, 9H, 'Boc-C(CH<sub>3</sub>)<sub>3</sub>). <sup>13</sup>C NMR (125 MHz, CDCl<sub>3</sub>) δ 174.01, 162.21, 156.80 (3 × C=O), 145.07 (C-2), 144.86, 132.59, 129.91, 128.02 (Ar-C), 109.92 (C-3), 80.60 ('Boc-C(CH<sub>3</sub>)<sub>3</sub>), 72.56 (C-9), 68.53 (C-7), 67.90 (C-8), 52.38 (C-6), 50.19 (C-4), 48.68 (C-5), 28.26 ('Boc-C(CH<sub>3</sub>)<sub>3</sub>), 22.86, 21.63 (COCH<sub>3</sub>, PhCH<sub>3</sub>). HR-MS (ESI) calcd. for C<sub>24</sub>H<sub>35</sub>N<sub>2</sub>O<sub>11</sub>S [M+H]<sup>+</sup>, 559.1962; found 559.1966.

**Methyl 5-acetamido-7,8-di-O-acetyl-9-azido-2,6-anhydro-4-[2,3-bis(tert-butoxycarbonyl)guanidino]-3,4,5-trideoxy-D-glycero-D-galacto-non-2-enonate (23).**

Compound **21** (200 mg, 1 eq) was dissolved in 3 mL acetone-water (2:1) and NaN<sub>3</sub> (117 mg, 5 eq) was added. The solution was heated at 67 °C under N<sub>2</sub> for two days. After completion, the solution was concentrated and purified by flash chromatography to give 100 mg compound **22** (crude product, 75%) which was used in the next step without further purification. The crude product was dissolved in 2 mL anhydrous DCM, and 200 μL TFA was added. The solution was kept stirring at room temperature until no starting material remained. Solvent was then removed under vacuum and the residue was dissolved in 2 mL anhydrous DCM, and TEA (140 μL, 4 eq) was added. After the solution was cooled down to 0 °C, N,N'-Di-Boc-1H-pyrazole-1-carboximidine (150 mg, 2 eq) was added. The reaction mixture was allowed to warm up to room temperature and kept stirring overnight. After completion, the reaction was quenched with water and extracted with ethyl acetate. The organic phase was washed with brine, dried over Na<sub>2</sub>SO<sub>4</sub>, concentrated and purified by flash chromatography to give the desired product. 108 mg (82%). <sup>1</sup>H NMR (500 MHz, CDCl<sub>3</sub>) δ 8.63, 8.15, 7.70, 6.43 (2 × d, 2 × brs, 4 H, 2 × NH, 2 × OH), 5.82 (d, *J* = 2.4 Hz, 1H, H-3), 5.20 (ddd, *J* = 10.2, 8.1, 2.4 Hz, 1H, H-4), 4.22 – 4.15 (m, 2H, H-6, H-5), 4.02 (td, *J* = 10.2, 6.1 Hz, 1H, H-8),

3.72 (dd,  $J = 12.6, 2.8$  Hz, 1H, H-9), 3.60 – 3.53 (m, 2H, H-9', H-7), 2.04 (s, 3H, COCH<sub>3</sub>), 1.52 (2 × s, 2 × 9H, 2 × 'Boc-C(CH<sub>3</sub>)<sub>3</sub>). <sup>13</sup>C NMR (125 MHz, CDCl<sub>3</sub>) δ 174.04, 162.29, 162.08, 157.56 (4 × C=O), 152.70 (C=N), 146.31 (C-2), 107.51 (C-3), 84.39, 80.11 (2 × 'Boc-C(CH<sub>3</sub>)<sub>3</sub>), 69.14 (C-6), 54.89 (C-9), 52.53 (C-7), 51.53 (C-8), 48.33 (C-5), 28.23, 28.04 (2 × 'Boc-C(CH<sub>3</sub>)<sub>3</sub>), 22.96 (COCH<sub>3</sub>). HR-MS (ESI) calcd. for C<sub>23</sub>H<sub>38</sub>N<sub>7</sub>O<sub>10</sub> [M+H]<sup>+</sup>, 572.2680; found 572.2681.

**Methyl 5-acetamido-9-(4-biphenyl-1H-1,2,3-triazol-1-yl)-4-[2,3-bis(tert-butoxycarbonyl)guanidino]-2,6-anhydro-4-[2,3-bis(tert-butoxycarbonyl)guanidino]-3,4,5-trideoxy-D-glycero-D-galacto-non-2-enonate (24).** Compound **23** (200 mg, 1 eq) and 4-ethynylbiphenyl (32 mg, 1.5 eq) were reacted following the protocol above to provide the desired product. 180 mg (69%). <sup>1</sup>H NMR (700 MHz, CDCl<sub>3</sub>) δ 8.55, 8.06 (2 × d, 2H, 2 × NH), 7.94 (s, 1H, triazole-H), 7.81 (d,  $J = 8.3$  Hz, 2H, Ar-H), 7.57 (dd,  $J = 13.1, 7.8$  Hz, 4H, Ar-H), 7.39 (t,  $J = 7.7$  Hz, 2H, Ar-H), 7.31 (t,  $J = 7.4$  Hz, 1H, Ar-H), 5.75 (d,  $J = 2.3$  Hz, 1H, H-3), 5.51 (brs, 1H, OH), 5.16 – 5.10 (m, 1H, H-4), 4.90 (dd,  $J = 14.0, 1.7$  Hz, 1H, H-9), 4.54 (dd,  $J = 14.0, 6.7$  Hz, 1H, H-9'), 4.48 – 4.43 (m, 1H, H-8), 4.20 (d,  $J = 10.4$  Hz, 1H, H-6), 3.96 (td,  $J = 10.4, 6.2$  Hz, 1H, H-5), 3.69 (s, 3H, COOCH<sub>3</sub>), 3.34 (d,  $J = 9.0$  Hz, 1H, H-7), 1.90 (s, 3H), 1.47, 1.43 (2 × s, 2 × 9H, 2 × 'Boc-C(CH<sub>3</sub>)<sub>3</sub>). <sup>13</sup>C NMR (176 MHz, CDCl<sub>3</sub>) δ 174.10, 162.26, 162.03, 157.37 (4 × C=O), 152.66 (C=N), 146.98 (C-2), 146.26 (triazole-C4), 121.69 (triazole-C5), 140.63, 140.43, 129.41, 128.77, 127.37, 126.86, 125.99 (Ar-C), 107.54 (C-3), 84.22, 79.96 (2 × 'Boc-C(CH<sub>3</sub>)<sub>3</sub>), 69.33 (C-6), 68.54 (C-4), 53.90 (C-9), 52.42 (C-8), 51.58 (C-7), 48.37 (C-5), 28.17, 27.99 ('Boc-C(CH<sub>3</sub>)<sub>3</sub>), 22.86 (COCH<sub>3</sub>). HR-MS (ESI) calcd. for C<sub>37</sub>H<sub>48</sub>N<sub>7</sub>O<sub>10</sub> [M+H]<sup>+</sup>, 750.3463; found 750.3454.

**General Procedure for Synthesis of Compounds 25a-d.** A solution of compound **19** (1 eq) and TEA (3 eq) in anhydrous DCM was cooled to 0 °C and the corresponding anhydride or acyl chloride (3 eq) was added dropwise. The resulting mixture was warmed to room temperature and

kept stirring overnight. After completion, the reaction was quenched with water and extracted with ethyl acetate. The organic layer was collected and washed with saturated NaHCO<sub>3</sub>, brine, and sequentially and dried with NaSO<sub>4</sub>. Solvents were removed under reduced pressure and the residue was separated by flash chromatography to give the desired crude products. For hydrolysis of the C1-methyl ester, the crude product was dissolved in MeOH, and 0.5 M NaOH was added. The mixture was kept stirring at room temperature. After completion, the pH was adjusted to 2 with Amberlite IR-120 (H<sup>+</sup>). The solution was then filtered and purified by flash chromatography to provide the desired products with yields of 42%-68% (over two steps).

**5-Acetamido-2,6-anhydro-4-propionamido-3,4,5-trideoxy-D-glycero-D-galacto-non-2-enonic acid (25a).** 28 mg (68%, over two steps). <sup>1</sup>H NMR (500 MHz, CD<sub>3</sub>OD) δ 5.49 (d, *J* = 2.0 Hz, 1H, H-3), 4.75 (dd, *J* = 9.7, 2.0 Hz, 1H, H-4), 4.20 (d, *J* = 10.8 Hz, 1H, H-6), 4.10-4.06 (m, 1H, H-5), 3.86-3.85 (m, 1H, H-8), 3.79 (dd, *J* = 11.4, 3.0 Hz, 1H, H-9), 3.63 (dd, *J* = 11.4, 5.4 Hz, 1H, H-9'), 3.55 (d, *J* = 9.0 Hz, 1H, H-7), 2.17 (q, *J* = 7.6 Hz, 2H, α-CH<sub>2</sub>), 1.93 (s, 3H, COCH<sub>3</sub>), 1.09 (t, *J* = 7.6 Hz, 3H, β-CH<sub>3</sub>). <sup>13</sup>C NMR (125 MHz, CD<sub>3</sub>OD) δ 177.40, 174.17 (2 × C=O), 106.15 (C-3), 77.49 (C-6), 71.46 (C-8), 70.05 (C-7), 64.88 (C-9), 49.64 (C-5), 30.40 (α-CH<sub>2</sub>), 22.78 (COCH<sub>3</sub>), 10.59 (β-CH<sub>3</sub>). HR-MS (ESI) calcd. for C<sub>14</sub>H<sub>21</sub>N<sub>2</sub>O<sub>8</sub> [M-H]<sup>-</sup>, 345.1298; found 345.1302

**5-Acetamido-2,6-anhydro-4-pentanamido-3,4,5-trideoxy-D-glycero-D-galacto-non-2-enonic acid (25b).** 25mg (56%, over two steps). <sup>1</sup>H NMR (500 MHz, CD<sub>3</sub>OD) δ 5.47 (d, *J* = 2.2 Hz, 1H, H-3), 4.76 (dd, *J* = 9.8, 2.2 Hz, 1H, H-4), 4.19 (d, *J* = 10.8 Hz, 1H, H-6), 4.09 -4.05 (m, 1H, H-5), 3.87-3.85 (m, 1H, H-8), 3.78 (dd, *J* = 11.5, 3.1 Hz, 1H, H-9), 3.66 (dd, *J* = 11.5, 5.1 Hz, 1H, H-9'), 3.57 (t, *J* = 7.8 Hz, 1H, H-7), 2.17 (t, *J* = 7.5 Hz, 2H, α-CH<sub>2</sub>), 1.94 (s, 3H, COCH<sub>3</sub>), 1.60 – 1.51 (m, 2H, β-CH<sub>2</sub>), 1.34-1.29 (m, 2H, γ-CH<sub>2</sub>), 0.90 (t, *J* = 7.4 Hz, 3H, δ-CH<sub>3</sub>). <sup>13</sup>C NMR (125 MHz, CD<sub>3</sub>OD) δ 176.55, 174.18, 170.01 (3 × C=O), 151.02 (C-2), 105.96 (C-3), 77.51 (C-

6), 71.55 (C-8), 69.91 (C-7), 64.71 (C-9), 49.60 (C-4), 49.00 (C-5), 37.02 ( $\alpha$ -CH<sub>2</sub>), 29.24 ( $\beta$ -CH<sub>2</sub>), 23.31 ( $\gamma$ -CH<sub>2</sub>), 23.31 (COCH<sub>3</sub>), 14.19 ( $\delta$ -CH<sub>3</sub>). HR-MS (ESI) calcd. for C<sub>16</sub>H<sub>25</sub>N<sub>2</sub>O<sub>8</sub> [M-H]<sup>-</sup>, 373.1611; found 373.1612.

**5-Acetamido-2,6-anhydro-4-cyclopropanecarboxamido-3,4,5-trideoxy-D-glycero-D-galacto-non-2-enonic acid (25c).** 22 mg (44%, over two steps). <sup>1</sup>H NMR (500 MHz, CD<sub>3</sub>OD)  $\delta$  5.54 (d,  $J$  = 2.1 Hz, 1H, H-3), 4.77 (dd,  $J$  = 9.8, 2.1 Hz, 1H, H-4), 4.20 (d,  $J$  = 10.7 Hz, 1H, H-6), 4.11-4.07 (m, 1H, H-5), 3.90 – 3.82 (m, 1H, H-8), 3.79 (dd,  $J$  = 11.4, 3.0 Hz, 1H, H-9), 3.66 (dd,  $J$  = 11.4, 5.2 Hz, 1H, H-9'), 3.57 (d,  $J$  = 9.0 Hz, 1H, H-7), 1.94 (s, 3H, COCH<sub>3</sub>), 1.58-1.53 (m, 1H,  $\alpha$ -CH), 0.88–0.78 (m, 2H,  $\beta$ -CH<sub>2</sub>), 0.74-0.72 (m, 2H,  $\beta$ -CH<sub>2</sub>). <sup>13</sup>C NMR (125 MHz, CD<sub>3</sub>OD)  $\delta$  176.90, 174.36, 169.54 (3  $\times$  C=O), 150.41 (C-2), 106.92 (C-3), 77.64 (C-6), 71.52 (C-8), 69.95 (C-7), 64.77 (C-9), 49.92 (C-4), 49.28 (C-5), 22.87 (COCH<sub>3</sub>), 15.05 ( $\alpha$ -CH), 7.57, 7.49 (2  $\times$   $\beta$ -CH<sub>2</sub>). HR-MS (ESI) calcd. for C<sub>15</sub>H<sub>21</sub>N<sub>2</sub>O<sub>8</sub> [M-H]<sup>-</sup>, 357.1298; found 357.1305.

**5-Acetamido-2,6-anhydro-4-cyclobutanecarboxamido-3,4,5-trideoxy-D-glycero-D-galacto-non-2-enonic acid (25d).** 19 mg (42%, over two steps). <sup>1</sup>H NMR (500 MHz, CD<sub>3</sub>OD)  $\delta$  5.49 (d,  $J$  = 2.2 Hz, 1H, H-3), 4.75 (dd,  $J$  = 9.8, 2.2 Hz, 1H, H-4), 4.21 (d,  $J$  = 10.8 Hz, 1H, H-6), 4.10-4.06 (m, 1H, H-5), 3.88-3.84 (m,  $m$ , 1H, H-8), 3.78 (dd,  $J$  = 11.5, 3.1 Hz, 1H, H-9), 3.66 (dd,  $J$  = 11.5, 5.2 Hz, 1H, H-9'), 3.56 (d,  $J$  = 9.3 Hz, 1H, H-7), 3.09-3.02 (m, 1H,  $\alpha$ -CH), 2.27 -1.77 (m, 6H, 3  $\times$  CH<sub>2</sub>), 1.93 (s, 3H, COCH<sub>3</sub>). <sup>13</sup>C NMR (125 MHz, CD<sub>3</sub>OD)  $\delta$  178.06, 174.20, 169.63 (3  $\times$  C=O), 150.52 (C-2), 106.54 (C-3), 77.53 (C-6), 71.55 (C-8), 69.94 (C-7), 64.77 (C-9), 49.57 (C-4), 49.14 (C-5), 40.90 ( $\alpha$ -CH), 26.44, 26.02, 19.09 (3  $\times$  CH<sub>2</sub>), 22.88 (COCH<sub>3</sub>). HR-MS (ESI) calcd. for C<sub>16</sub>H<sub>23</sub>N<sub>2</sub>O<sub>8</sub> [M-H]<sup>-</sup>, 371.1454; found 371.1458.

**Inhibition Assay.** Inhibition assays against 4MU-NANA cleavage and GM3 cleavage was performed using protocols reported previously.<sup>24</sup> NEU3 and NEU2 were expressed as N-terminal

MBP fusion proteins in *E. coli* and purified as previously reported.<sup>29</sup> NEU4 was expressed as an MBP fusion protein in *E. coli* and purified (see Supporting Information).<sup>18</sup>

NEU1 was overexpressed as a (His)<sub>6</sub> fusion protein in HEK293 cells, and used as a crude preparation from cell lysate.<sup>64</sup> The CathA-IRES-NEU1(His)<sub>6</sub> bicistronic recombinant plasmid was constructed by removing the hIL12 and CD19tmpk from pDy.hIL12.IRES.CD19tmpk.WS vector kindly provided J. Medin (University of Toronto Health Network) and replaced respectively by human Cathepsin A (CathA) and NEU1(His)<sub>6</sub> cDNA. The NEU1(His)<sub>6</sub> cDNA was PCR-amplified and inserted in the MCS of the pDy.hIL12.IRES.CD19tmpk.WS between the XbaI and BamHI sites. The CathA cDNA was PCR-modified and inserted into the MCS of pDy.hIL12.IRES.NEU1-GFP and pDy.hIL12.IRES.NEU1 between the EcoRI and AscI sites. All constructs were verified by PCR, enzymatic digestions and DNA sequencing. The final CathA-IRES-NEU1(His)<sub>6</sub> construct was assessed for sialidase activity in transfected HEK293T cells. The CathA-IRES-NEU1(His)<sub>6</sub> bicistronic HIV-1-based recombinant vesicular stomatitis virus glycoprotein-pseudotyped (VSVg) LV was generated by transient transfections of HEK293T cells by LV plasmid construct, packaging plasmid pCMVDR8.91 and the VSV-g envelope-coding plasmid pMD.G as described previously.<sup>65</sup> HEK293T cells were cultured in DMEM supplemented with 10% FBS, 1% streptomycin-penicillin at 37 °C in a humidified 5% CO<sub>2</sub> atmosphere. To overexpress NEU1, cells were transduced with CathA-IRES-NEU1(His)<sub>6</sub> lentivirus at 6 MOI in the presence of polybrene (8 µg mL<sup>-1</sup>). Five, 8 and 10 days after transduction, a portion of the cells was harvested to verify NEU1 expression by measuring acidic neuraminidase activity in the cell lysate. The transduced cells showed significantly higher neuraminidase activity in the cell lysates (76-85 nmol h<sup>-1</sup> mg<sup>-1</sup> of protein) as compared with the lysate of wild-type HEK293T cells (1.7-2.0 nmol h<sup>-1</sup> mg<sup>-1</sup> of protein).

All assays were conducted in 0.1 M sodium acetate buffer at optimum pH for each enzyme (pH 4.5 for NEU1, NEU3 and NEU4; pH 5.5 for NEU2).<sup>24</sup> To get comparable IC<sub>50</sub> values among the four isoenzymes, similar activity of each enzyme were used in the assay based on 4MU-NANA activity.

For assays using 4MU-NANA as the substrate, inhibitors in 3-fold serial dilutions were incubated with enzyme at 0 °C for 15 min. 4MU-NANA was then added to the mixture, making the final concentration of 4MU-NANA as 50 μM and the total volume of the reaction mixture as 20 μL. After incubation at 37 °C for 30 min, the reaction was quenched with 100 μL of 0.2 M sodium glycine buffer (pH 10.2). The reaction mixture was transferred to 386-well plate and the enzyme activity was determined by measuring fluorescence ( $\lambda_{\text{ex}} = 365 \text{ nm}$ ;  $\lambda_{\text{em}} = 445 \text{ nm}$ ) using a plate reader (Molecular Devices, Sunnyvale CA). Assays were performed with duplicates for each point and IC<sub>50</sub> was obtained by plotting the data with Graphpad Prism 7.0. For curves that showed less than a 50% decrease in signal, fits were conducted using maximum inhibition values found for DANA.

For inhibition assays against GM3 cleavage, a method developed by Markely and coworkers was adopted.<sup>66</sup> The assay was conducted in 0.1 M sodium acetate buffer (pH 4.5). After inhibitors in serial dilutions were incubated with enzyme at 0 °C for 15 min, GM3 was added, making the final concentration of GM3 500 μM and the total volume of the reaction mixture 20 μL. The reaction mixture was incubated at 37 °C for 30 min and quenched with 100 μL of freshly made 0.2 M sodium borate buffer (pH 10.2). 0.8% malononitrile solution (40 μL) was added to form a fluorescent adduct with the free sialic acid. Fluorescence was obtained ( $\lambda_{\text{ex}} = 357 \text{ nm}$ ;  $\lambda_{\text{em}} = 434 \text{ nm}$ ) and the data were processed using Graphpad Prism 7.0. For curves that showed less than a 50% decrease in signal, fits were conducted using maximum inhibition values found for DANA.

**$K_i$  Determinations.** Enzymes were incubated with inhibitors in serial dilutions at 0 °C for 15 min and serial concentrations of 4MU-NANA were added. The reaction mixture was transferred to a 386-well plate immediately and the rate of product formation was obtained by measuring fluorescence ( $\lambda_{\text{ex}} = 315 \text{ nm}$ ;  $\lambda_{\text{em}} = 450 \text{ nm}$ ) every 1 min for 30 min. The obtained data were processed with Graphpad Prism 7.0 for  $K_i$  determination.

**clogD<sub>7.4</sub> calculation.** The clogD<sub>7.4</sub> was calculated using MarvinSketch (Chemaxon, version 16.10.10.0). The consensus method was used with 0.1 M Cl<sup>-</sup> and 0.1 M Na<sup>+</sup> ions and pK<sub>a</sub> correction library.

**LogD<sub>7.4</sub> determination (shake-flask method).** Equal amounts of TRIS-HCl buffer (0.1 M, pH 7.4) and 1-octanol were mixed and vigorously shaken for 5 minutes to saturate the phases. The mixture was left until complete separation of the phases occurred and the buffer was retrieved. The stock solutions of test compounds (DMSO, 10 mM) were diluted to 10  $\mu\text{M}$  in saturated buffer (final DMSO concentration; 0.1 %). The buffer was transferred to a 96-well plate and saturated 1-octanol was added, resulting in a 40/140 and 30/150 1-octanol to water ratio, respectively (140/40 and 150/30 for compounds with clogD<sub>7.4</sub> below 0). Each ratio was measured in triplicate and simultaneous measurements were conducted with codeine as control. The plate was sealed with aluminum foil, shaken (1350 rpm, 25 °C, 2 h) on a Heidolph Titramax 1000 plate-shaker (Heidolph Instruments GmbH & Co. KG, Schwabach, Germany) and centrifuged (2000 rpm, 25 °C, 5 min, 5804 R Eppendorf centrifuge, Hamburg, Germany). The aqueous phase was transferred to a 96-well plate for analysis by liquid chromatography-mass spectrometry (LC-MS, see below). The logD<sub>7.4</sub> coefficients were calculated from the 1-octanol:buffer ratio (o:b), the initial concentration of the analyte in buffer (10  $\mu\text{M}$ ), and the concentration of the analyte in buffer ( $c_b$ ) with equation 1:

$$\log D_{7.4} = \log \left( \frac{10 \mu\text{M} - c_b}{c_b} \times \frac{1}{o:b} \right) \quad (\text{eq. 1})$$

**Parallel artificial membrane permeation assay.** Effective permeability ( $\log P_e$ ) was determined in a 96-well format with parallel artificial membrane permeation assay (PAMPA).<sup>45</sup> For each compound, measurements were performed at pH 7.4 in quadruplicate. Four wells of a deep well plate were filled with 500  $\mu\text{L}$  PRISMA HT buffer (pH 7.4, pION P/N 110 151). Then, analyte dissolved in DMSO (10 mM) was added to the buffer to yield 50  $\mu\text{M}$  solutions (containing 0.5 % DMSO). Afterwards, 200  $\mu\text{L}$  was transferred to each well of the donor plate of the PAMPA sandwich (pIon Billerica, USA, P/N 110 163). The filter membranes at the bottom of the acceptor plate were infused with 5  $\mu\text{L}$  of GIT-0 Lipid Solution (pIon, P/N 110 669) and 200  $\mu\text{L}$  of Acceptor buffer (pION, P/N 110 139) was filled into each acceptor well. The experiment was conducted with 10 % DMSO in PRISMA HT buffer and Acceptor buffer for compounds with insufficient solubility. The sandwich was assembled, placed in the GutBox<sup>TM</sup> (pION), and left undisturbed for 16 h. Then, it was disassembled and the compound concentration of donor, acceptor and reference compartment was measured by LC-MS (see below). Effective permeability ( $\log P_e$ ) was calculated from the compound flux deduced from the concentration in the donor and acceptor compartment as well as the retention in the filter area with the aid of the PAMPA Explorer Software (pIon, version 3.5).

**Metabolic stability in human liver microsomes.** Incubations were performed in triplicate in a 96-well format on an Eppendorf Thermomixer Comfort. The reaction mixture (270  $\mu\text{L}$ ) consisting of liver microsomes, TRIS-HCl buffer (0.1 M, pH 7.4) and  $\text{MgCl}_2$  (2 mM) was preheated (37  $^\circ\text{C}$ , 500 rpm, 10 min), and the incubation was initiated by adding 30  $\mu\text{L}$  of compound solution (200  $\mu\text{M}$ ) in TRIS-HCl buffer. The final concentration of the compound was 20  $\mu\text{M}$ , including 0.5 mg  $\text{mL}^{-1}$  human liver microsomes. At the beginning of the experiment ( $t = 0$  min) and after an

incubation time of 10, 30, 60, and 90 min, samples (40  $\mu\text{L}$ ) were transferred to 120  $\mu\text{L}$  of ice cold MeOH and centrifuged (3700 rpm, 4  $^{\circ}\text{C}$ , 10 min). Then, 80  $\mu\text{L}$  of supernatant was transferred to a 96-well plate for analysis by LC-MS (see below). The metabolic half-life ( $t_{1/2}$ ) was calculated from the slope of the linear regression from the log percentage remaining compound versus incubation time relationship. Control experiments were performed in parallel with control substance as positive control or containing 1 mM bis(4-nitrophenyl) phosphate (esterase inhibitor, negative control). Compounds with  $t_{1/2} > 90$  min were considered to be metabolically stable.

**Colorectal adenocarcinoma (Caco-2) cell permeation assay.** Cultivation, splitting, seeding of Caco-2 cells as well as the assay protocol previously described by Schönemann et al.<sup>39</sup> Permeation assays were conducted in triplicate at a concentration of 62.5  $\mu\text{M}$  containing 0.6% DMSO. Samples (40  $\mu\text{L}$ ) were withdrawn after 30 min, analyzed by LC-MS (see below) and the apparent permeation ( $P_{app}$ ) was calculated according to equation 4. The compound flux (mol/s) is  $dQ/dt$ ,  $A$  is the surface area of the monolayer ( $\text{cm}^2$ ) and  $c_0$  is the initial concentration.]

$$P_{app} = \frac{dQ}{dt} \times \frac{1}{A \times c_0} \quad (\text{eq. 2})$$

Compounds with a  $P_{app} < 2 \times 10^{-6}$  cm/s are considered as low permeable according to Hou *et al.* (2007).<sup>42, 46</sup>

**Solubility.** A sample of 5  $\mu\text{L}$  of predesolved compounds (DMSO, 10 mM) were added to 500  $\mu\text{L}$  of buffer (Tris-HCl 0.1 M pH7.4;  $\mu\text{L}$  PRISMA HT buffer; pH 7.4, pION P/N 110 151) and water containing 0.9% NaCl) ending in 1 % DMSO. The vials were put into super-sonic bath (Branson 2510, Danbury, USA) for 30 min at 25  $^{\circ}\text{C}$  and then left at 25  $^{\circ}\text{C}$  for 24 h to equilibrate. The dispersion was filtered (0.2  $\mu\text{m}$ ), diluted in MeOH and analyzed by LC-MS (see below).

**Liquid chromatography-mass spectrometry measurements (LC-MS).** Analyses were performed using a 1100/1200 Series HPLC System coupled to a 6410 Triple Quadrupole mass detector (Agilent Technologies, Inc., Santa Clara, CA, USA) equipped with electrospray ionization. The system was controlled with the Agilent MassHunter Workstation Data Acquisition software (version B.03.01). The column used was an Atlantis® T3 C18 column (2.1 x 50 mm) with a 3 µm-particle size (Waters Corp., Milford, MA, USA). The mobile phase consisted of eluent A: 0.1 % formic acid in water and eluent B: MeCN containing 0.1% formic acid. The flow rate was maintained at 0.6 mL/min. The gradient was ramped from 95% A/5% B to 5% A/95% B over 1 min, and then hold at 5% A/95% B for 0.1 min. The system was then brought back to 95% A/5% B, resulting in a total duration of 4 min. Fragmentor voltage and collision energy were optimized for the analysis of compounds in multiple reaction monitoring mode in positive mode. The concentrations of the analytes were quantified by the Agilent Mass Hunter Quantitative Analysis software (version B.04.00).

**Molecular Dynamics (MD) Simulations.** MD simulations were run for the inhibitor **8b** bound to NEU2, NEU3, and NEU4. Inhibitor **8b** was simulated in its zwitterionic form, i.e. as a carboxylate at C1 and as a guanidinium at C4. For simulations with NEU2, we used the crystal structure of NEU2 bound to **1** (PDB: 1VCU)<sup>27</sup> as a starting structure for the enzyme. The non-terminal residues G227, E228, S284, G295, P286, and G287 were added to the crystal structure for NEU2 using Modeller in Chimera.<sup>59,67-69</sup> We used our previously reported homology model for NEU3,<sup>29,30</sup> and we used the SWISS-MODEL website<sup>70-74</sup> to generate a homology model for NEU4 based on the 1VCU structure.<sup>27</sup> The portion of NEU4 between N289 and F368 is not homologous to NEU2; therefore, residues 290–367 (78 in total) were removed from the NEU4 model before running MD simulations. The coordinates for **8b** were based on those of **6** bound to NEU2 (PDB ID: 2F0Z)<sup>50</sup>

with the biphenyl-triazole and hydrogens added in Avogadro.<sup>75, 76</sup> To obtain the initial position for **8b** in the active site of Neu2, we aligned it to **6** in the crystal structure 2F0Z,<sup>50</sup> and we kept the active site waters for our simulations. For simulations with NEU3 and NEU4, each enzyme was aligned separately with the starting structure for NEU2 using the MatchMaker tool in Chimera.<sup>59, 68, 69</sup> The starting positions for **8b** in the active sites of NEU2, NEU3, and NEU4 are shown in Supporting Information.

All simulations were run in AMBER 15<sup>77</sup> using *pmemd.cuda* (GPU acceleration) on Nvidia GeForce GTX 980 GPUs. The *ff14SB* force field<sup>78</sup> was used for NEU2, NEU3, and NEU4, while the general AMBER force field (GAFF)<sup>79</sup> was used for **8b**. Partial charges for **8b** were assigned using the AM1 with bond charge correction (AM1-BCC) model<sup>80</sup> in the *antechamber* module of AmberTools15.<sup>77</sup> The enzyme-inhibitor complexes with NEU2 and NEU3 were neutralized with the addition of Na<sup>+</sup> ions, and that for NEU4 were neutralized with the additions of Cl<sup>-</sup> ions. All complexes were solvated in a box of TIP3P water<sup>81</sup> with 10 Å between the solute and the edges of the box in all three dimensions. For all systems, the water was first minimized using 100 steps of steepest decent, followed by 4900 steps of conjugate gradient. Then the entire system was minimized with 100 steps of steepest decent, followed by 4900 steps of conjugate gradient. The systems were further equilibrated by heating from 5 K to 300 K over 50 ps, followed by cooling back to 5 K over an additional 50 ps. After the annealing step, the systems were again heated from 5 K to 300 K over 100 ps, then allowed to run at 300 K for 100 ps before the production simulations were started. Production was run for 50 ns. The time step was 2 fs, bonds to hydrogen were constrained with the SHAKE<sup>82</sup> algorithm, and the cutoff for non-bonded interactions was 8.0 Å. The temperature was maintained with the Berendsen thermostat<sup>83</sup> (*ntt* = 1) with velocities rescaled

every 1 ps. The final 25-ns of the simulations were used for analysis with the *cpptraj* module of AmberTools15.<sup>77, 84</sup>

**Neuraminidase Assay in Mouse Brain Tissue.** Mice with targeted disruption of the *neu1* (*neu1<sup>-/-</sup>*), *neu3* (*neu3<sup>-/-</sup>*) and *neu4* (*neu4<sup>-/-</sup>*) genes have been previously described<sup>55, 57, 85</sup>. Mice with a combined deficiency of NEU4 and NEU3 were obtained by intercrossing *neu4* and *neu3* knockout (KO) mouse strains.<sup>85</sup> Mice were housed in an enriched environment with continuous access to food and water, under constant temperature and humidity, on a 12 h light:dark cycle. Approval for the animal care and the use in the experiments was granted by the Animal Care and Use Committee of the Ste-Justine University Hospital Research Center.

At the age of 12 weeks, mice were sacrificed using a CO<sub>2</sub> chamber and their brains extracted, snap-frozen with liquid nitrogen and kept at -80 °C. For measurement of neuraminidase activity 100 mg of frozen brain tissue was homogenized in water in a ratio of 100 mg of tissue per 500 µL of water in the 1.5 mL Eppendorf tubes using Kontes Pellet motorized pestle. Protein concentration in the homogenate was measured by the Bradford method using the Bio-Rad reagent. Acidic α-neuraminidase activity was assayed at pH 4.6 using fluorogenic 4-methylumbelliferyl-N-acetyl neuraminic acid (4MU-NANA) substrate as previously described.<sup>55</sup> The reaction mixture contained an aliquot of homogenate corresponding to 300 µg of total protein, neuraminidase inhibitor in a concentration of 0-150 µM and substrate in a final concentration of 200 µM. The reaction was carried on at 37 °C for 30 min after which it was terminated by the addition of 1900 µL of 0.4 M glycine buffer, pH 10.5. For blank samples, the reaction mixture contained buffer, inhibitor and substrate only but the same volume of homogenate was added after the termination of reaction.

## ASSOCIATED CONTENT

**Supporting Information.**  $^1\text{H}$  and  $^{13}\text{C}$  NMR data, HR-MS data, and HPLC traces for intermediates and final products,  $\text{IC}_{50}$  curves and  $K_i$  determinations. This material is available free of charge via the Internet at <http://pubs.acs.org>

## AUTHOR INFORMATION

### Corresponding Author

E-mail: [ccairo@ualberta.ca](mailto:ccairo@ualberta.ca)

### Author Contributions

TG synthesized and characterized all compounds unless otherwise noted, conducted  $\text{IC}_{50}$  and  $K_i$  measurements and wrote the manuscript; PG synthesized compounds **25a-d**; CZ and RZ developed and implemented protein purification protocols; MRR performed molecular modeling and analysis and wrote the manuscript; PD and BE designed and conducted PK analysis and wrote the manuscript; AF produced HEK293 cells expressing NEU1; ED and AP designed and performed inhibition experiments in murine brain homogenate, analyzed data, and wrote the manuscript; CWC designed experiments, interpreted data, and wrote the manuscript.

## ACKNOWLEDGEMENTS

This work was supported by a grant from the Canadian Glycomics Network (GlycoNet), and the Natural Sciences and Engineering Research Council of Canada (NSERC).

## ABBREVIATIONS

NEU, neuraminidase enzyme; Neu5Ac, 5-acetamino-3,5-dideoxy-D-glycero-D-galacto-non-2-ulosonic acid; DANA, 2-deoxy-2,3-didehydro-N-acetylneuraminic acid; 4MU-NANA, 2'-(4-

methylumbellifery)- $\alpha$ -D-*N*-acetylneuraminic acid; SAR, structure-activity relationship; CuAAC, copper-catalyzed azide–alkyne cycloaddition; C9-BA-DANA, C9-(butyl-*N*-amide) DANA; C9-4HMT-DANA, C9-(4-hydroxymethyltriazolyl) DANA

## REFERENCES

1. Angata, T.; Varki, A. Chemical diversity in the sialic acids and related  $\alpha$ -keto acids: An evolutionary perspective. *Chem. Rev.* **2002**, *102*, 439-470.
2. Chen, X.; Varki, A. Advances in the biology and chemistry of sialic acids. *ACS Chem. Biol.* **2010**, *5*, 163-176.
3. Varki, A. Sialic acids in human health and disease. *Trends. Mol. Med.* **2008**, *14*, 351-360.
4. Buschiazzo, A.; Alzari, P. M. Structural insights into sialic acid enzymology. *Curr. Opin. Chem. Biol.* **2008**, *12*, 565-572.
5. Miyagi, T.; Yamaguchi, K. Mammalian sialidases: Physiological and pathological roles in cellular functions. *Glycobiology* **2012**, *22*, 880-896.
6. Seyrantepe, V.; Poulpetova, H.; Froissart, R.; Zobot, M.-T. Z.; Marie, I.; Pshezhetsky, A. V. Molecular pathology of NEU1 gene in sialidosis. *Hum. Mutat.* **2003**, *22*, 343-352.
7. Kwak, J. E.; Son, M.-Y.; Son, Y. S.; Son, M. J.; Cho, Y. S. Biochemical and molecular characterization of novel mutations in GLB1 and NEU1 in patient cells with lysosomal storage disorders. *Biochem. Biophys. Res. Commun.* **2015**, *457*, 554-560.
8. Gayral, S.; Garnotel, R.; Castaing-Berthou, A.; Blaise, S.; Fougerat, A.; Berge, E.; Montheil, A.; Malet, N.; Wymann, M. P.; Maurice, P.; Debelle, L.; Martiny, L.; Martinez, L. O.; Pshezhetsky, A. V.; Duca, L.; Laffargue, M. Elastin-derived peptides potentiate atherosclerosis through the immune Neu1-PI3K gamma pathway. *Cardiovasc. Res.* **2014**, *102*, 118-127.
9. Yang, A.; Gyulay, G.; Mitchell, M.; White, E.; Trigatti, B. L.; Igdoura, S. A. Hypomorphic sialidase expression decreases serum cholesterol by downregulation of VLDL production in mice. *J. Lipid. Res.* **2012**, *53*, 2573-2585.
10. Miyagi, T.; Takahashi, K.; Hata, K.; Shiozaki, K.; Yamaguchi, K. Sialidase significance for cancer progression. *Glycoconj. J.* **2012**, *29*, 567-577.
11. Takahashi, K.; Hosono, M.; Sato, I.; Hata, K.; Wada, T.; Yamaguchi, K.; Nitta, K.; Shima, H.; Miyagi, T. Sialidase NEU3 contributes neoplastic potential on colon cancer cells as a key modulator of gangliosides by regulating Wnt signaling. *Int. J. Cancer* **2015**, *137*, 1560-1573.
12. Shiga, K.; Takahashi, K.; Sato, I.; Kato, K.; Saijo, S.; Moriya, S.; Hosono, M.; Miyagi, T. Upregulation of sialidase NEU3 in head and neck squamous cell carcinoma associated with lymph node metastasis. *Cancer Sci.* **2015**, *106*, 1544-1553.
13. Silvestri, I.; Testa, F.; Zappasodi, R.; Cairo, C. W.; Zhang, Y.; Lupo, B.; Galli, R.; Di Nicola, M.; Venerando, B.; Tringali, C. Sialidase NEU4 is involved in glioblastoma stem cell survival. *Cell Death Dis* **2014**, *5*, e1381.

14. Hyun, S. W.; Liu, A.; Liu, Z.; Cross, A. S.; Verceles, A. C.; Magesh, S.; Kommagalla, Y.; Kona, C.; Ando, H.; Luzina, I. G.; Atamas, S. P.; Piepenbrink, K. H.; Sundberg, E. J.; Guang, W.; Ishida, H.; Lillehoj, E. P.; Goldblum, S. E. The NEU1-selective sialidase inhibitor, C9-butylamide-DANA, blocks sialidase activity and NEU1-mediated bioactivities in human lung in vitro and murine lung in vivo. *Glycobiology* **2016**, *26*, 834-849.
15. Cairo, C. W. Inhibitors of the human neuraminidase enzymes. *MedChemComm* **2014**, *5*, 1067-1074.
16. von Itzstein, M. The war against influenza: Discovery and development of sialidase inhibitors. *Nat. Rev. Drug. Discov.* **2007**, *6*, 967-974.
17. Hata, K.; Koseki, K.; Yamaguchi, K.; Moriya, S.; Suzuki, Y.; Yingsakmongkon, S.; Hirai, G.; Sodeoka, M.; von Itzstein, M.; Miyagi, T. Limited inhibitory effects of oseltamivir and zanamivir on human sialidases. *Antimicrob. Agents. Chemother.* **2008**, *52*, 3484-3491.
18. Albohy, A.; Mohan, S.; Zheng, R. B.; Pinto, B. M.; Cairo, C. W. Inhibitor selectivity of a new class of oseltamivir analogs against viral neuraminidase over human neuraminidase enzymes. *Bioorg. Med. Chem. Lett.* **2011**, *19*, 2817-2822.
19. Li, Y.; Cao, H.; Yu, H.; Chen, Y.; Lau, K.; Qu, J.; Thon, V.; Sugiarto, G.; Chen, X. Identifying selective inhibitors against the human cytosolic sialidase NEU2 by substrate specificity studies. *Mol. Biosyst.* **2011**, *7*, 1060-1072.
20. Magesh, S.; Savita, V.; Moriya, S.; Suzuki, T.; Miyagi, T.; Ishida, H.; Kiso, M. Human sialidase inhibitors: Design, synthesis, and biological evaluation of 4-acetamido-5-acylamido-2-fluoro benzoic acids. *Bioorganic Med. Chem.* **2009**, *17*, 4595-4603.
21. This compound has been previously named as a C9-butyl N-amide derivative of DANA (C9-BA-DANA). This could more appropriately be named as a C9-pentylamide, but we maintain the previous nomenclature for consistency with the literature.
22. Magesh, S.; Moriya, S.; Suzuki, T.; Miyagi, T.; Ishida, H.; Kiso, M. Design, synthesis, and biological evaluation of human sialidase inhibitors. Part 1: Selective inhibitors of lysosomal sialidase (NEU1). *Bioorg. Med. Chem. Lett.* **2008**, *18*, 532-537.
23. Khedri, Z.; Li, Y.; Cao, H.; Qu, J.; Yu, H.; Muthana, M. M.; Chen, X. Synthesis of selective inhibitors against *V. cholerae* sialidase and human cytosolic sialidase NEU2. *Org. Biomol. Chem.* **2012**, *10*, 6112-6120.
24. Zhang, Y.; Albohy, A.; Zou, Y.; Smutova, V.; Pshezhetsky, A. V.; Cairo, C. W. Identification of selective inhibitors for human neuraminidase isoenzymes using C4,C7-modified 2-deoxy-2,3-didehydro-N-acetylneuraminic acid (DANA) analogues. *J. Med. Chem.* **2013**, *56*, 2948-2958.
25. Zou, Y.; Albohy, A.; Sandbhor, M.; Cairo, C. W. Inhibition of human neuraminidase 3 (NEU3) by C9-triazole derivatives of 2,3-didehydro-N-acetyl-neuraminic acid. *Bioorg. Med. Chem. Lett.* **2010**, *20*, 7529-7533.

26. Albohy, A.; Zhang, Y.; Smutova, V.; Pshezhetsky, A. V.; Cairo, C. W. Identification of selective nanomolar inhibitors of the human neuraminidase, NEU4. *ACS Med. Chem. Lett.* **2013**, *4*, 532-7.
27. Chavas, L. M. G.; Tringali, C.; Fusi, P.; Venerando, B.; Tettamanti, G.; Kato, R.; Monti, E.; Wakatsuki, S. Crystal structure of the human cytosolic sialidase Neu2 - Evidence for the dynamic nature of substrate recognition. *J. Biol. Chem.* **2005**, *280*, 469-475.
28. Buchini, S.; Gallat, F.-X.; Greig, I. R.; Kim, J.-H.; Wakatsuki, S.; Chavas, L. M. G.; Withers, S. G. Tuning mechanism-based inactivators of neuraminidases: Mechanistic and structural Insights. *Angew. Chem. Int. Ed. Engl.* **2014**, *126*, 3450-3454.
29. Albohy, A.; Li, M. D.; Zheng, R. B.; Zou, C.; Cairo, C. W. Insight into substrate recognition and catalysis by the human neuraminidase 3 (NEU3) through molecular modeling and site-directed mutagenesis. *Glycobiology* **2010**, *20*, 1127-1138.
30. Albohy, A.; Richards, M. R.; Cairo, C. W. Mapping substrate interactions of the human membrane-associated neuraminidase, NEU3, using STD NMR. *Glycobiology* **2015**, *25*, 284-293.
31. Magesh, S.; Suzuki, T.; Miyagi, T.; Ishida, H.; Kiso, M. Homology modeling of human sialidase enzymes NEU1, NEU3 and NEU4 based on the crystal structure of NEU2: Hints for the design of selective NEU3 inhibitors. *J. Mol. Graph.* **2006**, *25*, 196-207.
32. Meldal, M.; Tornøe, C. W. Cu-catalyzed azide-alkyne cycloaddition. *Chem. Rev.* **2008**, *108*, 2952-3015.
33. Lu, Y.; Gervay-Hague, J. Synthesis of C-4 and C-7 triazole analogs of zanamivir as multivalent sialic acid containing scaffolds. *Carbohydr. Res.* **2007**, *342*, 1636-1650.
34. Shidmoosavee, F. S.; Watson, J. N.; Bennet, A. J. Chemical insight into the emergence of influenza virus strains that are resistant to Relenza. *J. Am. Chem. Soc.* **2013**, *135*, 13254-13257.
35. Staudinger, H.; Meyer, J. Über neue organische phosphorverbindungen III. phosphinmethylenderivate und phosphinimine. *Helvetica Chimica Acta* **1919**, *2*, 635-646.
36. Potier, M.-C.; Mameli, L.; Bélisle, M.; Dallaire, L.; Melancon, S. B. Fluorometric assays of neuraminidase with a sodium (4-methylumbellifery- $\alpha$ -D-N-acetylneuraminate) substrate. *Anal. Biochem.* **1979**, *94*, 287-296.
37. Warner, T. G.; O'Brien, J. S. Synthesis of 2'-(4-methylumbelliferyl)- $\alpha$ -D-N-acetylneuraminic acid and detection of skin fibroblast neuraminidase in normal humans and in sialidosis. *Biochemistry* **1979**, *18*, 2783-2787.
38. Monti, E.; Bassi, M. T.; Papini, N.; Riboni, M.; Manzoni, M.; Venerando, B.; Croci, G.; Preti, A.; Ballabio, A.; Tettamanti, G.; Borsani, G. Identification and expression of NEU3, a novel human sialidase associated to the plasma membrane. *Biochem. J.* **2000**, *349*, 343-351.

39. Schönemann, W.; Kleeb, S.; Dätwyler, P.; Schwaradt, O.; Ernst, B. Prodruggability of carbohydrates — Oral FimH antagonists. *Can. J. Chem* **2016**, *94*, 909-919.
40. Schade, D.; Kotthaus, J.; Riebling, L.; Kotthaus, J.; Müller-Fielitz, H.; Raasch, W.; Hoffmann, A.; Schmidtke, M.; Clement, B. Zanamivir amidoxime- and N-hydroxyguanidine-based prodrug approaches to tackle poor oral bioavailability. *J. Pharm. Sci.* **2015**, *104*, 3208-3219.
41. Seebach, D.; Thaler, A.; Blaser, D.; Ko, S. Y. Transesterifications with 1,8-diazabicyclo[5.4.0]undec-7-ene/lithium Bromide (DBU/LiBr) – Also applicable to cleavage of peptides from resins in merrifield syntheses. *Helvetica Chimica Acta* **1991**, *74*, 1102-1118.
42. Hou, T.; Wang, J.; Zhang, W.; Xu, X. ADME evaluation in drug discovery. 7. Prediction of oral absorption by correlation and classification. *J. Chem. Inf. Model* **2007**, *47*, 208-218.
43. Kah, M.; Brown, C. D. LogD: Lipophilicity for ionisable compounds. *Chemosphere* **2008**, *72*, 1401-1408.
44. OECD. Guideline for Testing of Chemicals, no.107: Partition Coefficient (n-octanol/water), Shake Flask Method. 1995.
45. Kansy, M.; Senner, F.; Gubernator, K. Physicochemical high throughput screening: Parallel artificial membrane permeation assay in the description of passive absorption processes. *J. Med. Chem.* **1998**, *41*, 1007-1010.
46. Avdeef, A.; Bendels, S.; Di, L. i.; Faller, B.; Kansy, M.; Sugano, K.; Yamauchi, Y. PAMPA—Critical factors for better predictions of absorption. *J. Pharm. Sci.* **2007**, *96*, 2893-2909.
47. Amidon, G. L.; Lennernäs, H.; Shah, V. P.; Crison, J. R. A theoretical basis for a biopharmaceutic drug classification: The correlation of in vitro drug product dissolution and in vivo bioavailability. *Pharm. Res.* **1995**, *12*, 413-420.
48. Custodio, J. M.; Wu, C.-Y.; Benet, L. Z. Predicting drug disposition, absorption/elimination/transporter interplay and the role of food on drug absorption. *Adv. Drug Deliv. Rev.* **2008**, *60*, 717-733.
49. Hubatsch, I.; Ragnarsson, E. G. E.; Artursson, P. Determination of drug permeability and prediction of drug absorption in Caco-2 monolayers. *Nat. Protocols* **2007**, *2*, 2111-2119.
50. Chavas, L. M. G., Kato, R., McKimm-Breschkin, J., Colman, P.M., Fusi, P., Tringali, C., Venerando, B., Tettamanti, G., Monti, E., Wakatsuki, S. Crystal structure of the human sialidase NEU2 in complex with zanamivir inhibitor (PDB ID: 2F0Z).
51. Conformational nomenclature for five and six-membered ring forms of monosaccharides and their derivatives. *Eur. J. Biochem.* **1980**, *111*, 295-298.

52. Fushinobu, S. Cremer-Pople parameter calculator. <http://enzyme13.bt.a.u-tokyo.ac.jp/CP/> (July 6, 2017).
53. Chavas, L. M. G.; Tringali, C.; Fusi, P.; Venerando, B.; Tettamanti, G.; Kato, R.; Monti, E.; Wakatsuki, S. Crystal structure of the human cytosolic sialidase Neu2 - Evidence for the dynamic nature of substrate recognition. *J. Biol. Chem.* **2005**, *280*, 469-475.
54. Woods, R. J.; Grant, O. C.; Makeneni, S.; Foley, B. L. The effect of substrate presentation and activation on neuraminidase NEU2 specificity. *The FASEB Journal* **2017**, *31*, 1b111.
55. Seyrantepe, V.; Canuel, M.; Carpentier, S.; Landry, K.; Durand, S.; Liang, F.; Zeng, J.; Caqueret, A.; Gravel, R. A.; Marchesini, S.; Zwingmann, C.; Michaud, J.; Morales, C. R.; Levade, T.; Pshezhetsky, A. V. Mice deficient in Neu4 sialidase exhibit abnormal ganglioside catabolism and lysosomal storage. *Hum. Mol. Genet.* **2008**, *17*, 1556-68.
56. Seyrantepe, V.; Hinek, A.; Peng, J.; Fedjaev, M.; Ernest, S.; Kadota, Y.; Canuel, M.; Itoh, K.; Morales, C. R.; Lavoie, J.; Tremblay, J.; Pshezhetsky, A. V. Enzymatic activity of lysosomal carboxypeptidase (cathepsin) A is required for proper elastic fiber formation and inactivation of endothelin-1. *Circulation* **2008**, *117*, 1973-81.
57. Yamaguchi, K.; Shiozaki, K.; Moriya, S.; Koseki, K.; Wada, T.; Tateno, H.; Sato, I.; Asano, M.; Iwakura, Y.; Miyagi, T. Reduced susceptibility to colitis-associated colon carcinogenesis in mice lacking plasma membrane-associated sialidase. *PloS one* **2012**, *7*, e41132.
58. Koseki, K.; Wada, T.; Hosono, M.; Hata, K.; Yamaguchi, K.; Nitta, K.; Miyagi, T. Human cytosolic sialidase NEU2-low general tissue expression but involvement in PC-3 prostate cancer cell survival. *Biochem. Biophys. Res. Commun.* **2012**, *428*, 142-9.
59. Yang, Z.; Lasker, K.; Schneidman-Duhovny, D.; Webb, B.; Huang, C. C.; Pettersen, E. F.; Goddard, T. D.; Meng, E. C.; Šali, A.; Ferrin, T. E. UCSF Chimera, MODELLER, and IMP: An integrated modeling system. *J. Struct. Biol.* **2012**, *179*, 269-278.
60. Smutova, V.; Albohy, A.; Pan, X.; Korchagina, E.; Miyagi, T.; Bovin, N.; Cairo, C. W.; Pshezhetsky, A. V. Structural basis for substrate specificity of mammalian neuraminidases. *PloS one* **2014**, *9*, e106320.
61. Varghese, J. N.; Chandana Epa, V.; Colman, P. M. Three - dimensional structure of the complex of 4 - guanidino - Neu5Ac2en and influenza virus neuraminidase. *Protein Science* **1995**, *4*, 1081-1087.
62. von Itzstein, M.; Wu, W.-Y.; Jin, B. The synthesis of 2,3-didehydro-2,4-dideoxy-4-guanidinyl-N-acetylneuraminic acid: A potent influenza virus sialidase inhibitor. *Carbohydr. Res.* **1994**, *259*, 301-305.
63. von Itzstein, M.; Wu, W.-Y.; Kok, G. B.; Pegg, M. S.; Dyason, J. C.; Jin, B.; Phan, T. V.; Smythe, M. L.; White, H. F.; Oliver, S. W.; Colman, P. M.; Varghese, J. N.; Ryan, D. M.;

- Woods, J. M.; Bethell, R. C.; Hotham, V. J.; Cameron, J. M.; Penn, C. R. Rational design of potent sialidase-based inhibitors of influenza virus replication. *Nature* **1993**, *363*, 418-423.
64. Pshezhetsky, A. V.; Potier, M. Association of N-acetylgalactosamine-6-sulfate sulfatase with the multienzyme lysosomal complex of  $\beta$ -galactosidase, cathepsin A, and neuraminidase: Possible implication for intralysosomal catabolism of keratan sulfate. *J. Biol. Chem.* **1996**, *271*, 28359-28365.
65. Yoshimitsu, M.; Sato, T.; Tao, K.; Walia, J. S.; Rasaiah, V. I.; Sleep, G. T.; Murray, G. J.; Poepl, A. G.; Underwood, J.; West, L. Bioluminescent imaging of a marking transgene and correction of Fabry mice by neonatal injection of recombinant lentiviral vectors. *Proc. Natl. Acad. Sci. U.S.A.* **2004**, *101*, 16909-16914.
66. Markely, L. R. A.; Ong, B. T.; Hoi, K. M.; Teo, G.; Lu, M. Y.; Wang, D. I. C. A high-throughput method for quantification of glycoprotein sialylation. *Anal. Biochem.* **2010**, *407*, 128-133.
67. Šali, A.; Blundell, T. L. Comparative protein modelling by satisfaction of spatial restraints. *J. Mol. Biol.* **1993**, *234*, 779–815.
68. Resource for Biocomputing, Visualization, and Informatics,. *UCSF Chimera*, candidate version 1.11; University of California, San Francisco (supported by NIGMS P41-GM103311), 2016.
69. Pettersen, E. F.; Goddard, T. D.; Huang, C. C.; Couch, G. S.; Greenblatt, D. M.; Meng, E. C.; Ferrin, T. E. UCSF Chimera – A visualization system for exploratory research and analysis. *J. Comput. Chem.* **2004**, *25*, 1605–1612.
70. Swiss Institute of Bioinformatics. SWISS-MODEL. <https://swissmodel.expasy.org/interactive> (July 6, 2016).
71. Biasini, M.; Bienert, S.; Waterhouse, A.; Arnold, K.; Studer, G.; Schmidt, T.; Kiefer, F.; Cassarino, T. G.; Bertoni, M.; Bordoli, L.; Schwede, T. SWISS-MODEL: Modelling protein tertiary and quaternary structure using evolutionary information. *Nucleic Acids Res.* **2014**, *42*, W252–W258.
72. Kiefer, F.; Arnold, K.; Künzli, M.; Bordoli, L.; Schwede, T. The SWISS-MODEL Repository and associated resources. *Nucleic Acids Res.* **2009**, *37*, D387–D392.
73. Bordoli, L.; Kiefer, F.; Arnold, K.; Benkert, P.; Battey, J.; Schwede, T. Protein structure homology modeling using SWISS-MODEL workspace. *Nat. Protocols* **2008**, *4*, 1–13.
74. Arnold, K.; Bordoli, L.; Kopp, J.; Schwede, T. The SWISS-MODEL workspace: a web-based environment for protein structure homology modelling. *Bioinformatics* **2006**, *22*, 195-201.
75. *Avogadro: An open-source molecular builder and visualization tool.*, Version 1.1.1, <http://avogadro.openmolecules.net/>; 2012.

76. Hanwell, M. D.; Curtis, D. E.; Lonie, D. C.; Vandermeersch, T.; Zurek, E.; Hutchison, G. R. Avogadro: An advanced semantic chemical editor, visualization, and analysis platform. *J. Cheminform.* **2012**, *4*, 17.
77. Case, D. A.; Berryman, J. T.; Betz, R. M.; Cerutti, D. S.; T.E. Cheatham III; Darden, T. A.; Duke, R. E.; Giese, T. J.; Gohlke, H.; Goetz, A. W.; Homeyer, N.; Izadi, S.; Janowski, P.; Kaus, J.; Kovalenko, A.; Lee, T. S.; LeGrand, S.; Li, P.; Luchko, T.; Luo, R.; Madej, B.; Merz, K. M.; Monard, G.; Needham, P.; Nguyen, H.; Nguyen, H. T.; Omelyan, I.; Onufriev, A.; Roe, D. R.; Roitberg, A.; Salomon-Ferrer, R.; Simmerling, C. L.; Smith, W.; Swails, J.; Walker, R. C.; Wang, J.; Wolf, R. M.; Wu, X.; York, D. M.; Kollman, P. A. *AMBER 15*, University of California: San Francisco, CA, 2015.
78. Hornak, V.; Abel, R.; Okur, A.; Strockbine, B.; Roitberg, A.; Simmerling, C. Comparison of multiple Amber force fields and development of improved protein backbone parameters. *Proteins* **2006**, *65*, 712–725.
79. Wang, J.; Wolf, R. M.; Caldwell, J. W.; Kollman, P. A.; Case, D. A. Development and testing of a general amber force field. *J. Comput. Chem.* **2004**, *25*, 1157–1174.
80. Jakalian, A.; Bush, B. L.; Jack, D. B.; Bayly, C. I. Fast, efficient generation of high-quality atomic charges. AM1-BCC model: I. Method. *J. Comput. Chem.* **2000**, *21*, 132–146.
81. Jorgensen, W. L.; Chandrasekhar, J.; Madura, J. D.; Impey, R. W.; Klein, M. L. Comparison of simple potential functions for simulating liquid water. *J. Chem. Phys.* **1983**, *79*, 926–935.
82. Ryckaert, J.-P.; Ciccotti, G.; Berendsen, H. J. C. Numerical integration of the cartesian equations of motion of a system with constraints: Molecular dynamics of n-alkanes. *J. Comput. Phys.* **1977**, *23*, 327–341.
83. Berendsen, H. J. C.; Postma, J. P. M.; Gunsteren, W. F. v.; DiNola, A.; Haak, J. R. Molecular dynamics with coupling to an external bath. *J. Chem. Phys.* **1984**, *81*, 3684–3690.
84. Roe, D. R.; Cheatham, T. E. PTRAJ and CPPTRAJ: Software for Processing and Analysis of Molecular Dynamics Trajectory Data. *J. Chem. Theory Comput.* **2013**, *9*, 3084–3095.
85. Pan, X.; De Aragao, C. B. P.; Velasco-Martin, J. P.; Priestman, D. A.; Wu, H. Y.; Takahashi, K.; Yamaguchi, K.; Sturiale, L.; Garozzo, D.; Platt, F. M.; Lamarche-Vane, N.; Morales, C. R.; Miyagi, T.; Pshezhetsky, A. V. Neuraminidases 3 and 4 regulate neuronal function by catabolizing brain gangliosides. *FASEB J* **2017**, *31*, 3467-3483.

## FIGURES

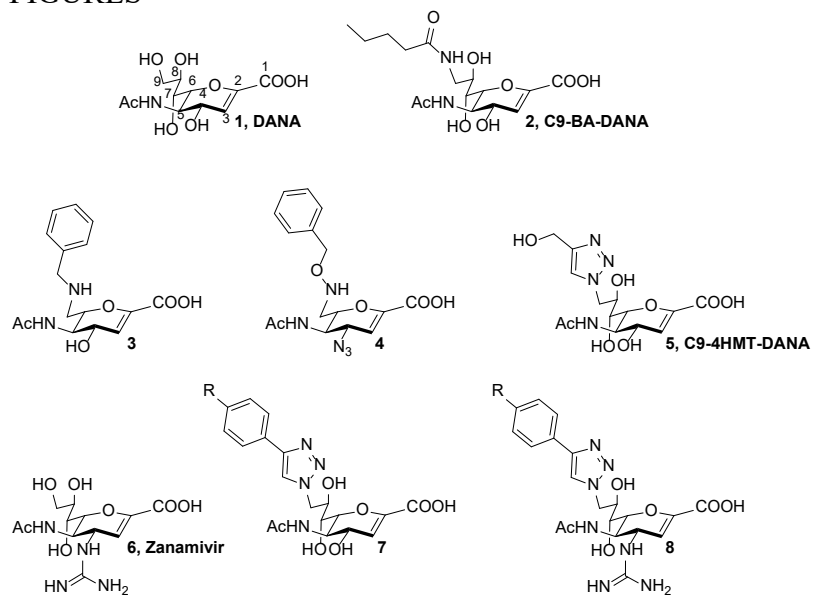


**Figure 1.** Inhibitor Targets

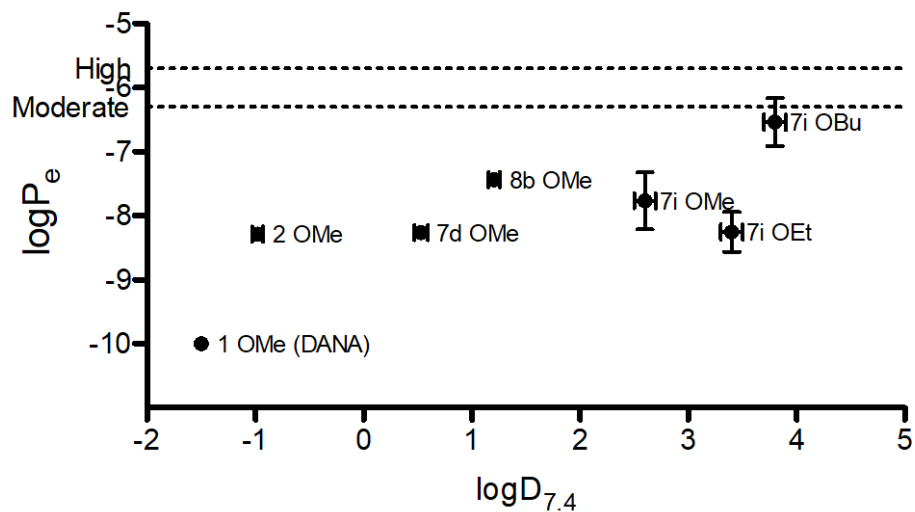


**Figure 2.** Passive permeability  $\log P_e$  of ester prodrugs versus lipophilicity. The dotted lines indicate the threshold for moderate and high absorption potential.<sup>46</sup> Error bars show the standard deviation of the measurement in six independent measurements of  $\log D_{7.4}$  and four independent measurements of  $\log P_e$ .

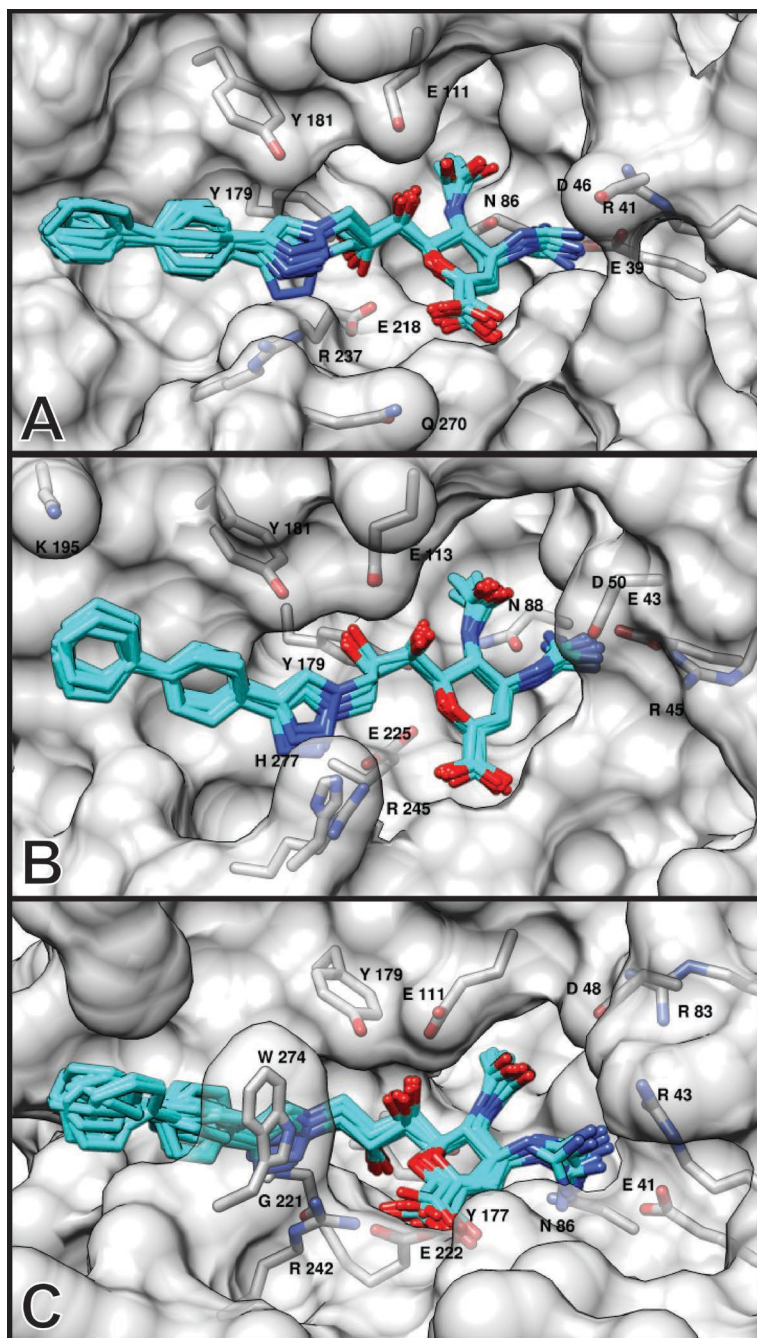


**Figure 3.** Average enzyme structures for A) NEU2, B) NEU3, and C) NEU4 with **8b** in the active site. The inhibitor is shown as 10 representative structures taken from the last 25 ns of the MD simulation.

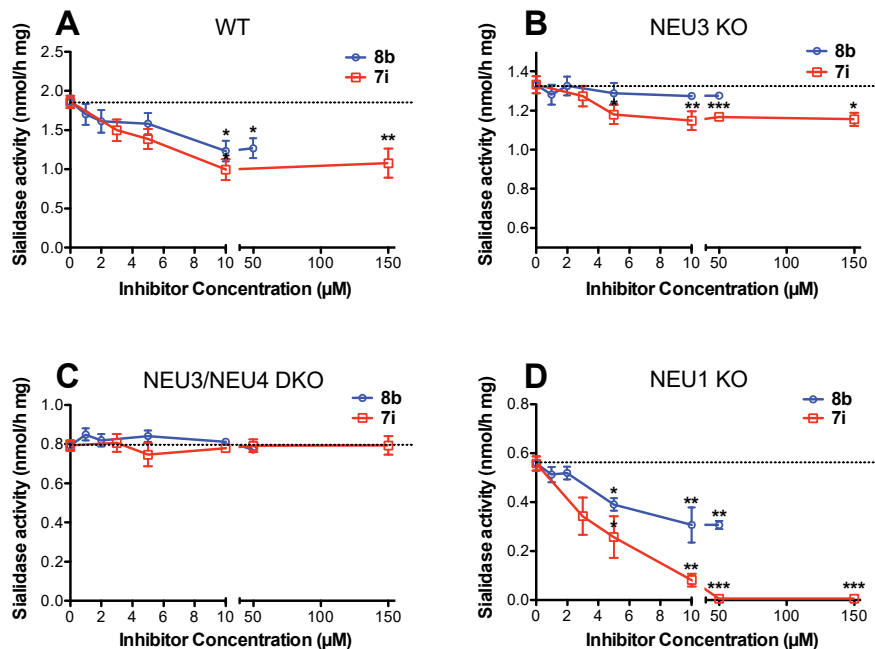
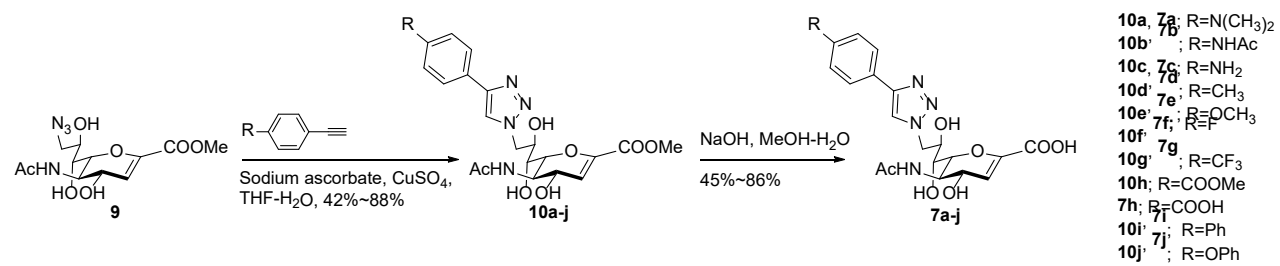
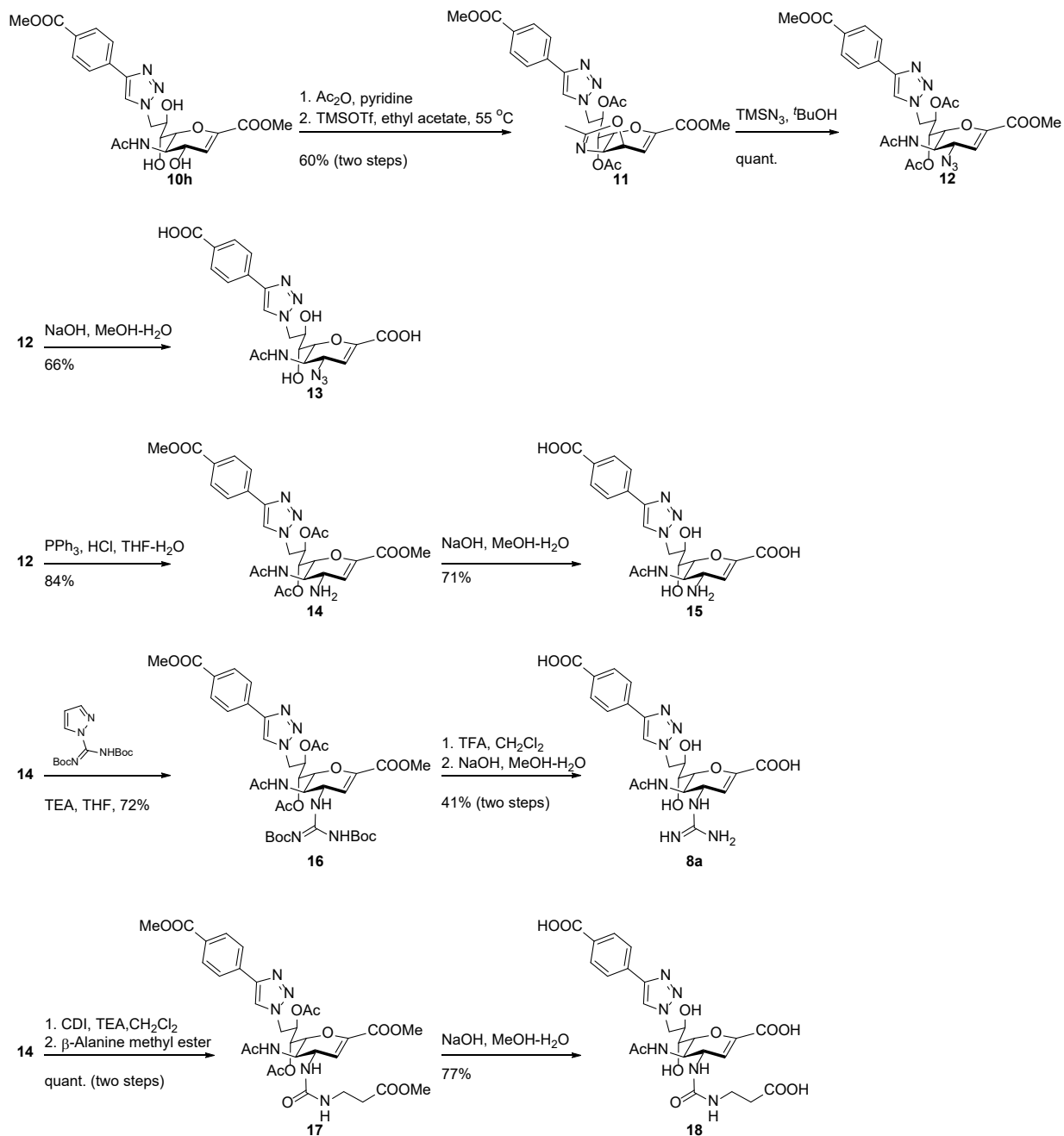


**Figure 4.** Inhibition of NEU activity in murine brain homogenate. Brains were extracted from WT C57Bl6 mice and those KO for the NEU1 (*neu1<sup>-/-</sup>*), NEU3 (*neu3<sup>-/-</sup>*), NEU4 (*neu4<sup>-/-</sup>*), or double KO (DKO) for the NEU3/4 genes (*neu3<sup>-/-</sup>; neu4<sup>-/-</sup>*). Brain homogenates were assayed for inhibition of neuraminidase activity against 4MU-NANA. The WT brain homogenates (A) showed partial inhibition (up to 70% at 10 µM) of neuraminidase activity by both **8b** and **7i**, while the NEU3 KO brain homogenate (B) showed no inhibition with **8b** and NEU3/4 DKO brain homogenate (C) showed no significant inhibition with either compound **8b** nor **7i**. The NEU1 KO brain homogenate (D) was the only sample to show dramatic inhibition for both compounds **8b** and **7i**, consistent with specificity of these compounds for the NEU3/4 isoenzymes. Importantly, all homogenates showed a complete inhibition of neuraminidase activity at 150 µM of DANA 1 (data not shown). Points are labeled as significantly different (\*,  $p < 0.05$ ; \*\*,  $p < 0.01$ ; and \*\*\*,  $p < 0.001$ ) from the activity in the absence of the inhibitors according to t-test with a Dunnett post-test. Data are shown as mean values  $\pm$  SD of 6 to 12 independent experiments.

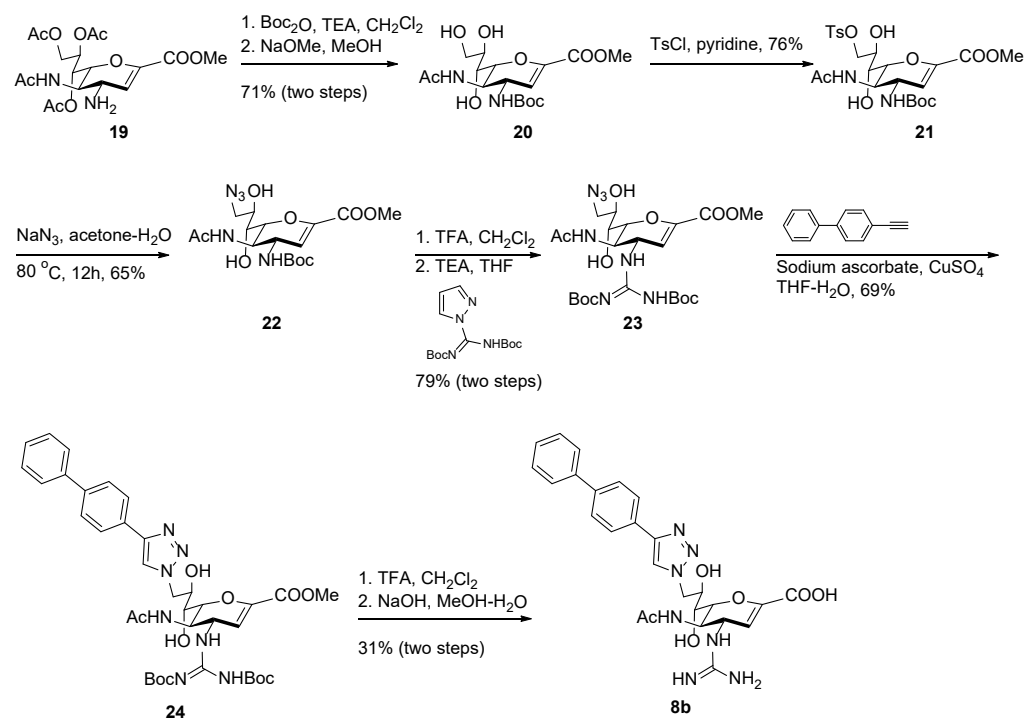
## SCHEMES



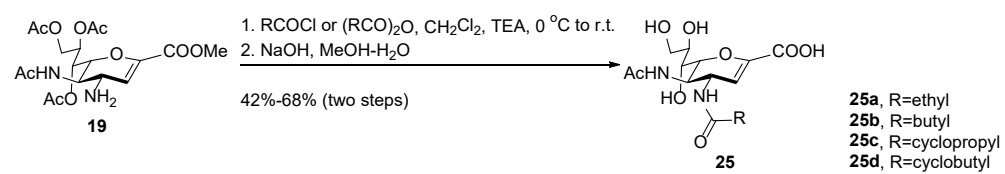
**Scheme 1.** Synthetic route to C9-phenyltriazole DANA analogues **7a-j**



**Scheme 2.** Synthetic routes to C4, C9-modified DANA analogues **8a**, **13**, **15**, **18**



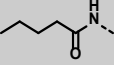
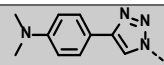
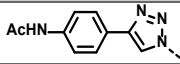
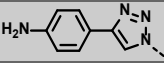
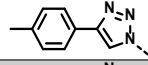
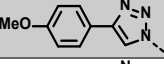
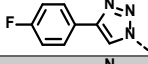
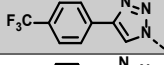
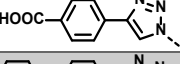
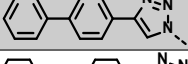
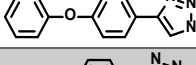
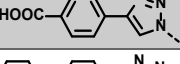
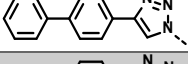
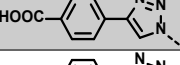
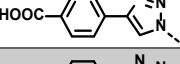
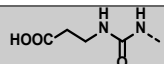
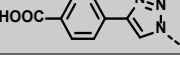
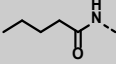
**Scheme 3.** Synthetic route to C4, C9-modified DANA analogue **8b**



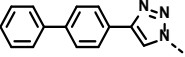
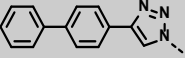
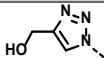
**Scheme 4.** Synthetic route to C4-amide DANA analogues **25a-d**

TABLES

**Table 1.** IC<sub>50</sub> data for NEU using 4MU-NANA as the substrate

Structure			IC <sub>50</sub> [μM]			
Compound	C4	C9	NEU1	NEU2	NEU3	NEU4
<b>1 (DANA)</b>	HO--	HO--	49 ± 8	37 ± 6	7.7 ± 0.8	8.3 ± 1.0
<b>2 (C9-BA-DANA)</b>	HO--		3.4 ± 0.2	>500	110 ± 40	220 ± 50
<b>6 (zanamivir)</b>		HO--	>500	7.8 ± 2.0	4.0 ± 0.6	47 ± 6
<b>7a</b>	HO--		190 ± 40	250 ± 40	9.3 ± 0.8	28 ± 3
<b>7b</b>	HO--		59 ± 5	78 ± 20	5.5 ± 0.5	11 ± 1
<b>7c</b>	HO--		76 ± 16	350 ± 90	8.7 ± 0.9	12 ± 1
<b>7d</b>	HO--		51 ± 7	290 ± 50	8.2 ± 1.3	3.9 ± 0.4
<b>7e</b>	HO--		47 ± 6	430 ± 200	5.9 ± 0.4	2.6 ± 0.3
<b>7f</b>	HO--		100 ± 40	>500	17 ± 2	1.3 ± 0.2
<b>7g</b>	HO--		140 ± 30	360 ± 50	3.3 ± 0.5	5.0 ± 0.9
<b>7h</b>	HO--		240 ± 90	110 ± 10	1.1 ± 0.1	3.0 ± 0.3
<b>7i</b>	HO--		>500	32 ± 5	0.70 ± 0.10	0.52 ± 0.10
<b>7j</b>	HO--		>500	84 ± 24	1.0 ± 0.1	0.97 ± 0.24
<b>8a</b>			>500	45 ± 5	0.61 ± 0.10	24 ± 2
<b>8b</b>			>500	5.9 ± 1.1	0.58 ± 0.14	5.9 ± 1.4
<b>13</b>	N <sub>3</sub> --		>500	>500	20 ± 6	400 ± 70
<b>15</b>	H <sub>2</sub> N--		>500	>500	>500	>500
<b>18</b>			>500	430 ± 300	>500	66 ± 16
<b>25a</b>		HO--	>500	>500	>500	>500
<b>25b</b>		HO--	>500	>500	>500	>500
<b>25c</b>		HO--	>500	>500	>500	>500
<b>25d</b>		HO--	>500	>500	>500	>500

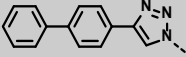
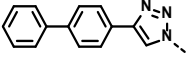
**Table 2.**  $K_i$  determinations

Structure			$K_i$ [ $\mu\text{M}$ ] <sup>a</sup>		
Compound	C4	C9	NEU2	NEU3	NEU4
<b>1 (DANA)</b>	HO--	HO--	25 ± 4	1.6 ± 0.3	5.8 ± 0.6
<b>6 (zanamivir)</b>		HO--	5.7 ± 1.5	0.62 ± 0.09	26 ± 4
<b>7i</b>	HO--		48 ± 9	0.28 ± 0.04	0.26 ± 0.04
<b>8b</b>			17 ± 4	0.32 ± 0.04	5 ± 1
<b>5<sup>b</sup></b>	HO--		ND	ND	0.030 ± 0.02

<sup>a</sup> None of these compounds showed significant activity towards NEU1, so only NEU2, NEU3, and NEU4 determinations were made.

<sup>b</sup> Previously reported data.<sup>26</sup>

**Table 3.** Inhibition of GM3 cleavage

Structure			$\text{IC}_{50}$ [ $\mu\text{M}$ ]			
Compound	C4	C9	NEU3	NEU4	Rel/NEU3 <sup>a</sup>	Rel/NEU4 <sup>a</sup>
<b>DANA (1)</b>	HO--	HO--	54 ± 10	26 ± 8	ND	ND
<b>7i</b>	HO--		12 ± 2	3.7 ± 0.7	4.1	7.0
<b>8b</b>			3.8 ± 0.5	ND	14	ND

<sup>a</sup> Relative activity as compared to DANA.

**Table 4.** Pharmacokinetic evaluation of C1-esters.

Parent compound	C1(O)R	clogD <sub>7.4</sub> <sup>a</sup>	logD <sub>7.4</sub> <sup>b</sup>	logP <sub>e</sub> [log cm s <sup>-1</sup> ] <sup>c</sup>	Solubility [μg mL <sup>-1</sup> ] <sup>d</sup>
<b>DANA, 1</b>	OMe	-3.31	< -1.5	nd	nd
<b>2</b>	OMe	-2.01	-1.0 ± 0.1	-8.3 ± 0.1	nd
<b>5</b>	OMe	-3.49	< -1.5	nd	nd
<b>8b</b>	OMe	-1.95	1.2 ± 0.1	-7.4 ± 0.1	nd
<b>7i</b>	OMe	0.91	2.3 ± 0.1	-7.8 ± 0.4*	Tris pH 7.4: 1.5 Prism pH 6.5: > 1.0 NaCl 0.9%: > 1.0
<b>7i</b>	OEt	1.27	3.4 ± 0.1	-8.3 ± 0.3*	Tris pH 7.4: 13.8 Prism pH 6.5: 3.2 NaCl 0.9%: 3.7
<b>7i</b>	OPr	1.79	nd	-8.2 ± 0.3*	Tris pH 7.4: 2.8 Prism pH 6.5: 1.7 NaCl 0.9%: 2.4
<b>7i</b>	OBu	2.23	3.8 ± 0.1	-6.5 ± 0.4*	Tris pH 7.4: 3.9 Prism pH 6.5: 3.2 NaCl 0.9%: 5.0

<sup>a</sup> clogD<sub>7.4</sub> was calculated using Marvin Sketch software (Version 16.10.10.0)

<sup>b</sup> Octanol-water distribution coefficients (logD<sub>7.4</sub>) were determined at pH 7.4 by a miniaturized shake flask procedure in sextuplicate in Tris buffer (0.1 M).

<sup>c</sup> P<sub>e</sub> = effective permeability: diffusion through an artificial membrane was determined by the parallel artificial membrane permeability assay (PAMPA) in quadruplicate at pH 6.5 in Prism buffer. Measurements indicated with \* indicate inclusive 10 % DMSO.

<sup>d</sup> The kinetic solubility was measured in singlet measurements in 3 different buffer systems (Tris 0.1 M, pH 7.4; Prism pH 6.5; 0.9 % NaCl in water).

**Table 5.** Cell permeability of **7i-OBu**.

	Caco2 P <sub>app</sub> after 30 min [10 <sup>-6</sup> cm s <sup>-1</sup> ] <sup>a</sup>			MetStab HLM 0.5 mg mL <sup>-1</sup> [min] <sup>b</sup>
	a-b	b-a	b-a/a-b	
<b>7i-OBu</b>	0.32 ± 0.09	2.2 ± 0.2	6.7	> 90

<sup>a</sup> P<sub>app</sub> = apparent permeability: permeation through a Caco-2 cell monolayer was assessed in the absorptive (a→b) and secretory (b→a) direction in triplicate. The initial compound concentration (c<sub>0</sub>) in the donor chamber was 62.5 μM.

<sup>b</sup> The metabolic stability assay was performed in human liver microsomes (HLM 0.5 mg mL<sup>-1</sup>) in triplicate.

TABLE OF CONTENTS GRAPHIC

